

CFD SIMULATION OF TRAIN FIRE IN THE ISTANBUL METRO TUNNEL

A THESIS SUBMITTED TO  
THE GRADUATE SCHOOL OF NATURAL AND APPLIED SCIENCES  
OF  
MIDDLE EAST TECHNICAL UNIVERSITY

BY

MAHİR İLTER BİLGE

IN PARTIAL FULFILLMENT OF THE REQUIREMENTS  
FOR  
THE DEGREE OF MASTER OF SCIENCE  
IN  
MECHANICAL ENGINEERING

JULY 2018



Approval of the thesis:

**CFD SIMULATION OF TRAIN FIRE IN THE ISTANBUL METRO TUNNEL**

submitted by **MAHİR İLTER BİLGE** in partial fulfillment of the requirements for the degree of **Master of Science in Mechanical Engineering Department, Middle East Technical University** by,

Prof. Dr. Halil Kalıpçılar  
Dean, Graduate School of **Natural and Applied Sciences** \_\_\_\_\_

Prof. Dr. M. A. Sahir Arıkan  
Head of Department, **Mechanical Engineering** \_\_\_\_\_

Prof. Dr. M. Halûk Aksel  
Supervisor, **Mechanical Engineering Department, METU** \_\_\_\_\_

**Examining Committee Members:**

Assoc. Prof. Dr. Ahmet Yozgatlıgil  
Mechanical Engineering Department, METU \_\_\_\_\_

Prof. Dr. M. Halûk Aksel  
Mechanical Engineering Department, METU \_\_\_\_\_

Assoc. Prof. Dr. Cüneyt Sert  
Mechanical Engineering Department, METU \_\_\_\_\_

Assist. Prof. Dr. Özgür Uğraş Baran  
Mechanical Engineering Department, METU \_\_\_\_\_

Assist. Prof. Dr. Onur Baş  
Mechanical Engineering Department, TEDU \_\_\_\_\_

**Date:** \_\_\_\_\_

**I hereby declare that all information in this document has been obtained and presented in accordance with academic rules and ethical conduct. I also declare that, as required by these rules and conduct, I have fully cited and referenced all material and results that are not original to this work.**

Name, Last Name: MAHİR İLTER BİLGE

Signature :

## **ABSTRACT**

### **CFD SIMULATION OF TRAIN FIRE IN THE ISTANBUL METRO TUNNEL**

Bilge, Mahir İlter

M.S., Department of Mechanical Engineering

Supervisor : Prof. Dr. M. Halûk Aksel

July 2018, 88 pages

Underground metro networks are expanding rapidly in all around the world and during the last few decades, tunnel fire accidents with severe casualties occurred in various countries. The frequency of the tunnel fire incidents will be increasing due to the increased amount of underground transportation routes in the upcoming years. In order to prevent the loss of lives in tunnel fires, accurate design of Tunnel Ventilation Systems is crucial.

This research thesis presents the simulation of a mid-train fire scenario in the tunnel of the Marmaray Metro Line by the use of Fire Dynamics Simulator (FDS) Computational Fluid Dynamics (CFD) Software. The main goal of the simulation is to determine the efficiency of the emergency ventilation system in case of a mid-train fire in the metro tunnels and investigate the ways to increase the safety degrees in underground metro tunnels.

Since mid-train fires are not widely studied, one purpose of this thesis is to attract attention to the risks associated with tunnel ventilation system activation in case of a

mid-tunnel fire.

In order to determine the boundary conditions of the CFD Simulation, on site measurements are carried out for the selected fire scenarios in the tunnel network. Full scale three dimensional tunnel geometry is modeled along with the five car train and the growth of fire is modeled by making use of appropriate approximations. Contour plots of temperature and visibility are obtained for the cases with and without the activation of Tunnel Ventilation Systems (TVS) and the tenability criterion in the tunnel was examined by making use of widely accepted standards.

By making a comparison of results with and without the TVS activation, it is concluded that during the mid-train tunnel fire, fan operation adversely effects the tenability conditions for the passengers at the downstream side of the fire. Therefore, for the studied fire scenario, it is safer to disable the ventilation fans and allow the passengers self-evacuate and activate the fans after evacuation to assist the fire-fighters.

**Keywords:** Tunnel Fire, Tunnel Ventilation, Fire Dynamics Simulator, Computational Fluid Dynamics

## ÖZ

### İSTANBUL METRO TÜNELİNDE TREN YANGINI SİMÜLYASYONU

Bilge, Mahir İlter

Yüksek Lisans, Makina Mühendisliği Bölümü

Tez Yöneticisi : Prof. Dr. M. Halûk Aksel

Temmuz 2018 , 88 sayfa

Dünya nüfusunun artması ve şehirlerin daha büyük hale gelmesi ile beraber, yer altı metro hatları genişlemekte ve yaygınlaşmaktadır. Son yıllarda meydana gelen can ve mal kaybına yola çan kazalar, metrolardaki tünel yangınının ne kadar tehlikeli olduğunu göstermektedir. Yaşanan olayların sıklığı, yer altı metro hatlarının genişlemesi ile beraber atacaktır. Tünel yangınlarında can kaybını önlemek için Tünel Havalandırma Sistemlerinin iyi bir şekilde tasarlanmış olması çok önemlidir

Bu tez çalışmasında, Fire Dynamics Simulator (FDS) Hesaplamalı Akışkanlar Dinamiği (HAD) Yazılımı kullanılarak, Marmaray Metro Hattının tüneline bir yangın senaryosunun simülasyonunu hazırlanmıştır. Simülasyonun ana amacı, metro tünellerinde yangın olması durumunda acil durum havalandırma sistemlerinin etkisini gözlemlemek ve tünellerdeki güvenlik derecesinin artırılmasının yollarını araştırmaktır.

İstanbul Metrosunda farklı noktalarda yapılan saha testlerinde tünel acil durum havalandırma sisteminin kapasitesi ölçülmüş ve ölçülen değerler HAD simülasyonunda

giriş koşulları olarak kullanılmıştır. Tam ölçekli üç boyutlu tünel geometrisi içerisinde beş vagonlu metro treni yerleştirilmiştir. Uygun yaklaşımlar kullanılarak yangının büyümesi modellenmiş ve tünel içerisindeki sıcaklık ve duman dağılımı incellenmiştir.

Tünel havalandırma sistemi çalışırken ve çalışmazken elde edilen sonuçlarda sıcaklık dağılımı ve görüş mesafesi grafikleri elde edilmiştir. Yapılan simülasyonların sonuçları incelendiğinde, özel bir koşul olan orta vagon yangını durumunda fan operasyonunun yolcu tahliyesini olumsuz etkilediği görülmüştür. Bu özel durumda acil durum havalandırma fanlarının kapatılması ve yolcuların bu şekilde tahliye edilmesi önerilmiştir.

Anahtar Kelimeler: Tünel Yangını, Tünel Havalandırma Sistemi, Fire Dynamics Simulator, Hesaplamalı Akışkanlar Dinamiği

To my parents...

## **ACKNOWLEDGMENTS**

First and foremost, I have to thank my advisor Prof. Dr. M. Halûk Aksel for the fruitful lectures of Fluid Dynamics and Computational Fluid Dynamics, during my undergraduate and graduate studies and also for his support during the course of the Master of Science study.

I also would like to thank to Thunderhead Engineering for providing the software of Pyrosim and Smokview for my academic studies.

I would also like to show my gratitude to Dr. Eren Musluoglu for his supportive ideas.

## TABLE OF CONTENTS

ABSTRACT . . . . .	v
ÖZ . . . . .	vii
ACKNOWLEDGMENTS . . . . .	x
TABLE OF CONTENTS . . . . .	xi
LIST OF TABLES . . . . .	xiv
LIST OF FIGURES . . . . .	xv
LIST OF SYMBOLS . . . . .	xviii
LIST OF ABBREVIATIONS . . . . .	xix
CHAPTERS	
1 INTRODUCTION . . . . .	1
1.1 General . . . . .	1
1.2 Previous Underground Tunnel Fires . . . . .	2
1.3 Aim of the Thesis . . . . .	4
1.4 Literature Survey on Tunnel Fire Studies . . . . .	5
1.5 Full Scale Tunnel Fire Tests . . . . .	17
1.6 Tunnel Ventilation Concept . . . . .	17

1.6.1	Longitudinal Ventilation . . . . .	19
1.6.2	Transverse Ventilation . . . . .	19
1.6.3	Critical Velocity in the Tunnel . . . . .	21
1.6.4	Critical Velocity in the Cross Passage . . . . .	22
1.7	Tenable Environment for Humans . . . . .	23
1.8	Description of Marmaray Tunnel . . . . .	26
2	MODELING OF FIRE . . . . .	29
2.1	Fire Dynamics Simulator . . . . .	30
2.1.1	Combustion Modeling Using Mixture Fraction . . . . .	31
2.1.1.1	Radiation Modeling Equations . . . . .	35
2.1.2	Limitations and Assumptions . . . . .	37
2.1.3	Visibility . . . . .	38
2.1.4	Validation of Fire Dynamics Simulation in Literature . . . . .	41
3	SITE MEASUREMENTS . . . . .	45
3.1	Tunnel Velocity Measurement . . . . .	45
3.2	Cross-Passage Velocity Measurement . . . . .	48
3.3	Measurement Method . . . . .	49
3.4	Results of Measurements . . . . .	50
4	SIMULATION . . . . .	53
4.1	Geometry . . . . .	53
4.1.1	Meshing . . . . .	55

4.1.2	Time Step . . . . .	57
4.1.3	Boundary Conditions . . . . .	58
4.2	Modeling of Fire . . . . .	59
4.2.1	Fire Growth . . . . .	59
4.2.2	Fire Characteristics . . . . .	60
5	SIMULATION RESULTS . . . . .	63
5.1	Validation Results . . . . .	63
5.2	Temperature Contours . . . . .	65
5.3	Contours of Visibility . . . . .	70
5.4	Temperature Graphs . . . . .	73
6	DISCUSSION AND CONCLUSION . . . . .	77
6.1	Discussion About the Results . . . . .	77
6.2	Recommendations for Future Work . . . . .	78
	REFERENCES . . . . .	81
APPENDICES		
A	TEST REPORTS . . . . .	83

## LIST OF TABLES

### TABLES

Table 1.1	Full Scale Tunnel Tests . . . . .	18
Table 1.2	Exposure Time to High Temperatures . . . . .	24
Table 2.1	Train Car Materials . . . . .	40
Table 2.2	Previously Used Soot Yield Values . . . . .	41
Table 3.1	Measured Tunnel Air Velocities . . . . .	51
Table 4.1	Boundary Conditions . . . . .	58
Table 4.2	Growth Factors Used In Previous Studies . . . . .	59

## LIST OF FIGURES

### FIGURES

Figure 1.1 Visualization of back layering in case of a fire in an enclosed tunnel with ventilation. Sketch by P. H. Thomas [27] . . . . .	6
Figure 1.2 Comparison of Smoke Distributions a) without Platform Screen Door and b) with Platform Screen Door [8] . . . . .	9
Figure 1.3 Test Set-up of Paris Metro by Stephane Gaillot [11] . . . . .	9
Figure 1.4 Smoke behavior in all 4 levels of Daegu Metro Station for 6 minutes [29] . . . . .	13
Figure 1.5 Pool fire set-up of Alper Çelik [32] . . . . .	13
Figure 1.6 Comparison of FDS Data with Experimental Data [10] . . . . .	16
Figure 1.7 Longitudinal Ventilation . . . . .	20
Figure 1.8 Transverse Ventilation . . . . .	20
Figure 1.9 Egress Route in Tunnel Fire in Case of a Fire at End Location . . .	21
Figure 1.10 Typical smoke distribution in a tunnel with cross passage [12] . . .	23
Figure 1.11 Stations of Marmaray Metro Line . . . . .	26
Figure 1.12 Marmaray Tunnel ventilation fan . . . . .	27
Figure 1.13 Smoke Test in Sirkeci Metro Station . . . . .	28
Figure 1.14 Marmaray Train . . . . .	28

Figure 2.1	State Relations for Propane . . . . .	33
Figure 3.1	Measurement locations on tunnel cross-section for 30 point layout .	47
Figure 3.2	Total and static pressure tubes . . . . .	47
Figure 3.3	Test set-up . . . . .	49
Figure 3.4	Cross passage velocity measurement . . . . .	50
Figure 4.1	Tunnel Cross Section . . . . .	55
Figure 4.2	CAD Model of Tunnel and Train . . . . .	56
Figure 4.3	Cross-Sectional View of the Mesh . . . . .	57
Figure 4.4	Heat Release Rate for Different Growth Factors . . . . .	60
Figure 4.5	Fire Location on the Train . . . . .	61
Figure 5.1	Experimental Setup of Scaled Tunnel . . . . .	64
Figure 5.2	Section View of Scaled Tunnel Model . . . . .	64
Figure 5.3	Comparison of FDS Results and Experimental Results . . . . .	65
Figure 5.4	Measurement Plane at $y = 3.7m$ . . . . .	66
Figure 5.5	Temperature Distribution at $y = 3.7m$ plane – a. with fan operation at $t = 120$ seconds, b. with no fan operation . . . . .	66
Figure 5.6	Temperature Distribution at $y = 3.7m$ plane – a. with fan operation at $t = 120$ seconds, b. with no fan operation . . . . .	67
Figure 5.7	Temperature Distribution at $y = 3.7m$ plane – a. with fan operation at $t = 120$ seconds, b. with no fan operation . . . . .	67
Figure 5.8	Temperature Distribution at $y = 3.7m$ plane – a. with fan operation at $t = 120$ seconds, b. with no fan operation . . . . .	68

Figure 5.9 Temperature Distribution at $y = 3.7m$ plane – a. with fan operation at $t = 120$ seconds, b. with no fan operation . . . . .	68
Figure 5.10 Visibility Plot at $y = 3.7m$ plane – a. with fan operation at $t = 120$ seconds, b. with no fan operation . . . . .	71
Figure 5.11 Visibility Plot at $y = 3.7m$ plane – a. with fan operation at $t = 120$ seconds, b. with no fan operation . . . . .	71
Figure 5.12 Visibility Plot at $y = 3.7m$ plane – a. with fan operation at $t = 120$ seconds, b. with no fan operation . . . . .	72
Figure 5.13 Visibility Plot at $y = 3.7m$ plane – a. with fan operation at $t = 120$ seconds, b. with no fan operation . . . . .	72
Figure 5.14 Visibility Plot at $y = 3.7m$ plane – a. with fan operation at $t = 120$ seconds, b. with no fan operation . . . . .	73
Figure 5.15 Comparison of Walkway Temperature Distribution With and With- out Fan Operation at 6 <sup>th</sup> Minute . . . . .	74
Figure 5.16 Comparison of Walkway Temperature Distribution With and With- out Fan Operation at 7 <sup>th</sup> Minute . . . . .	75
Figure A.1 Scenario Checklist 1 . . . . .	83
Figure A.2 Scenario Checklist 2 . . . . .	84
Figure A.3 Tunnel Velocity . . . . .	85
Figure A.4 Walkway Velocity . . . . .	86
Figure A.5 Cross Passage Velocity . . . . .	87
Figure A.6 Cold Flow Scenario . . . . .	88

## LIST OF SYMBOLS

$T_f$	Average temperature of fire site gasses [K]
$V_c$	Critical velocity [m/s]
$c$	Specific heat [kJ/kg · K]
$c_p$	Specific heat at constant pressure [kJ/kg.K]
$D_i$	Diffusion Coefficient
$D^*$	Characteristic Fire Diameter
$g$	Gravitational acceleration [m/s <sup>2</sup> ]
$H$	Height of duct or tunnel at fire site [m]
$k$	Thermal conductivity [W/m · K]
$K_g$	Grade Factor
$P$	Pressure [kPa]
$Q$	Heat release rate [kW]
$T$	Temperature [°C]
$t$	Time [s]
$u$	Velocity in x direction [m/s]
$v$	Velocity in y direction [m/s]
$w$	Width of opening of an enclosed space [m]
$\alpha$	Growth factor of fire [kW/s <sup>2</sup> ]
$\rho$	Density [kg/m <sup>3</sup> ]

## LIST OF ABBREVIATIONS

CFD	Computational Fluid Dynamics
DNS	Direct Numerical Simulation
FDS	Fire Dynamics Simulator
HVAC	Heating Ventilation and Air Conditioning
LES	Large Eddy Simulation
NFPA	National Fire Protection Association
OTE	Over Track Exhaust
RANS	Reynolds Averaged Navier Stokes
SES	Subway Environmental System
TVF	Tunnel Ventilation Fan
TVS	Tunnel Ventilation System



# CHAPTER 1

## INTRODUCTION

### 1.1 General

World's population is growing rapidly, and as the cities expand, the demand for public transportation is increasing. Increasing traffic problems in major cities force the municipalities to use railway systems in order to solve the problem. Underground transportation systems seem to be the best solution to solve the transportation problems in growing cities. Currently there are over 148 cities that use underground metro systems with over 1000km of network length and these numbers are increasing rapidly. As the underground systems become more frequent, the rate of accidents and emergency cases will tend to increase.

One of the most critical problems in underground systems are tunnel fires. Although the materials used in tunnels and train cars are fire rated, accidents involving fire and smoke cannot be prevented which causes numerous casualties as well as immense economic losses. The best way to fight fires in tunnels is to activate the tunnel ventilation system and remove the combustion products from the tunnel thus create a safe evacuation path for the passengers. Without adequate tunnel ventilation, smoke and heat tends to stay in the enclosed area and threatens the lives of hundreds of passengers and prevents the fire fighters to access the fire location.

There are various reasons for casualties in tunnel fires which include inhalation of combustion products, exposure to high heat fluxes and temperatures. The main reason of casualties in tunnel fires is not direct exposure to fire, but smoke inhalation due to

the hot air and toxic gasses. Moreover, as the smoke concentration in the air increases, visibility decreases and the passengers are unable to follow exit signs and find the evacuation path.

In order to create a smoke free path for the passengers, the smoke has to be pushed to the opposite direction of evacuation path. Therefore, tunnel ventilation systems have to be designed and engineered with great care and detailed analysis has to be carried out to predict the smoke movement in the tunnels and stations.

There are three modes of ventilation in subway systems. These modes are normal, congested and emergency modes. Normal operation mode is when the train is running as planned, the fresh air is mainly supplied by the piston effect of the incoming trains. Congested operation occurs when there is an operation problem with the trains. Such as a long delay which results in deficiency of ventilation in the station due to the lack of piston effect therefore decreases the comfort in the metro stations. During the congested mode, the ventilation fans operate to supply fresh air to the stations. The third mode of operation is the emergency operation which occurs due to a fire caused by malfunction of a train component or a baggage fire inside the station and creates the necessity of evacuation. In this case, the smoke extract fans start to operate and try to keep the evacuation routes in tenable conditions. This study investigates the emergency operation of the metro system, namely the Tunnel Ventilation System which is activated due to a fire case at the middle of the train.

## **1.2 Previous Underground Tunnel Fires**

Rail tunnel and station fires are often related to a baggage fire in the station, technical failure in the machinery, the restaurant area, electrical systems, HVAC system or it can be caused directly by an arson attack. These fires can be observed by the passengers and usually dealt with before the fire grows. Fires outside the train are more dangerous and they can occur for various reasons including the overheating of brakes or failure in hydraulic systems.

In a typical fire case in a metro tunnel, the fire starts with the ignition source and grows if there is sufficient amount of fuel and oxygen and it could progress to involve

an entire train car or multiple train cars.

Typical ignition sources for train fires can be:

- Arson attack,
- Electrical faults,
- Accident which results in derailment of the train,
- Overheating of hydraulic fluid.

Figures show that lots of catastrophes happened in underground transportation systems and a great deal of work needs to be carried out to prevent the loss of human lives in the future. The following points summarize the reasons of previous tunnel fires and the number of people who were affected.

- 1903 Paris Metro Train Fire

The short circuit in the engine caused ignition of the wooden metro train. The fire destroyed the circuit supplying the station lightning and the station was plunged into darkness. 84 people died at the Couronnes Metro Station.

- 1987 Kings Cross Station

A wooden escalator burned in the interchange station in London causing death of 31 people.

- 1994 New York Metro

An arsonist exploded a homemade bomb in a train car which was parked in a station and injured 48 people.

- 1995 Baku Metro

The fire initiated at the forth car, and it was caused by an electrical arc in the equipment. The train malfunctioned and stopped in the tunnel 200m away from the station. About 15 minutes after the ignition, the tunnel ventilation fans started operation and much of the smoke was drawn out through the evacuation path. 289 people died because of electrocution, smoke inhalation and high heat fluxes and 265 were injured.

- 1999 Mount Blanc

Mount Blanc is a road tunnel located between France and Italy. During a heavy goods vehicle fire, 38 people died and the fire could not be extinguished for 53 hours. The peak heat release rate is estimated to be over 380MW.

- 1999 Amsterdam High-Speed Train

The brakes of the train caught fire when it entered the Weesperplein Underground station. The fire entire station was filled with smoke and 2 people were injured.

- 2000 Kaprun Disaster

The hydraulic fluid under the train leaked to the electrical heater and caused a rapidly growing fire. Among the 167 people on the train only 12 people survived and 155 people died.

- 2001 St. Gotthard Tunnel Fire

Two trucks collided in a road tunnel and 11 people died. The fire burned for over 2 days.

- 2003 Daegu Subway Fire

An arson attack occurred in the metro station in South Korea. The arsonist spilled flammable liquid inside the train car and the fire spread to all train cars along with the non-incident train that stopped behind. 198 people died because the ventilation system was inadequate.

- Tsim Sha Tsui Station Hong Kong

An arsonist used a bottle of flammable liquid to start a fire. 18 people were injured, but majority of the people were unhurt because of the well-designed ventilation system.

### **1.3 Aim of the Thesis**

More people are using the underground transportation systems every year and more and more emergency cases will be reported with the widespread use of metro lines. Emergency ventilation systems have to be designed with care in order to prevent the loss of lives. The ventilation systems are deemed to be adequate if they prevent back layering and this is valid for the fires located at one end of the train. However during

a mid-train fire it is difficult to determine if the ventilation system assists or hinders the evacuation.

This thesis aims to assess the safety of the Marmaray Metro Line by making use of a scenario with the mid-train fire with the train located at the tunnel connection of the Ayrılıkçeşmesi Station. CFD method is used to simulate the fire since full scale tests are extremely costly for tunnel fires. Temperature and visibility contours are obtained with and without the ventilation system operation. These two scenarios are compared in order to observe the effects of tunnel ventilation system on the evacuation. The main purposes of this study includes:

- Assessing the emergency ventilation systems of the Istanbul Metro Stations and determining the ability of the system to control smoke and temperature inside the tunnel during a fire scenario,
- Determining the effect of tunnel ventilation systems during a mid-train tunnel fire,
- Making recommendations to improve the performance of emergency ventilation system for current and to be operated metro lines,
- Recommend future works in order to increase the engineering value of tunnel ventilation systems.

#### **1.4 Literature Survey on Tunnel Fire Studies**

Various scientists investigated the topic of tunnel fires, and its importance increased with the increasing number of tunnel fire incidents. Most of the researchers investigated critical velocity in tunnels and focused on ways of determining critical velocities for different fire sizes or tunnel geometries and this knowledge has reached a high level. Nowadays researchers are focusing on CFD simulations to assess the life safety of different metro stations and trying to find ways of increasing the safety levels by means of addition of fire suppression systems or revisions in tunnel ventilation systems.

Early studies on tunnel fires depended on experiments, such as the full scale tunnel

fire experiment carried out in Ofenegg Tunnel in 1965. Later on with the improvements in computers, more scientists adopted the method of numerical simulations. Although experimental studies are more accurate, they consume more time and they are extremely more expensive compared to CFD simulations.

In 1958, first scientific study about tunnel fires was carried out by Thomas [27]. By making use of simple energy equations he studied the back layering of hot smoke gases and carried out numerical analysis to equate the pressure gradient of chimney effect to the velocity head of inlet air. By making use of this calculation he calculated the velocity required to prevent back layering inside a tunnel.

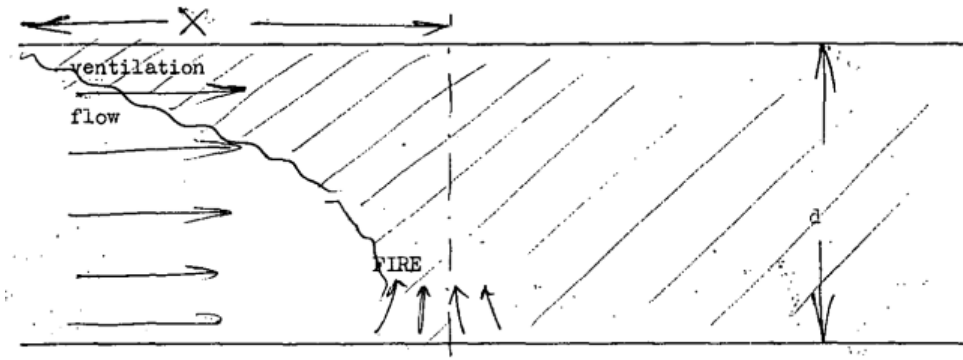


Figure 1.1: Visualization of back layering in case of a fire in an enclosed tunnel with ventilation. Sketch by P. H. Thomas [27]

Later on in 1968 [28], the author conducted experiments in a wind tunnel, investigated the behavior of smoke inside the ducts and came up with the concept of critical velocity. By equating the inertial forces to buoyant forces (Froude Number = 1), he obtained a relationship for critical velocity which is still being used by researchers. His conclusion was that the critical velocity is proportional to cube root of heat release rate. Thomas also compared his results with previous fire experiments and observed that the equation is a good approximation and the differences are due to the viscous effects which are neglected in his model. This empirical equation is called the Thomas Model.

One of the early studies was carried out in 1998 by Silas Li and William Kennedy [17] by making use of a commercial code on a DEC Alpha Workstation. An alternative ventilation system for the Buenos Aires Metro was suggested which consisted of jet fans located inside the tunnel on both ends of the station and 50m in to the

tunnel. With the conditions stated in the NFPA standard, the acceptance of the ventilation system was assessed by obtaining results of temperature and velocity. The train heat release rate used for the analysis was a low-intensity fire of  $1.8MW$  which corresponded to a train fire involving only the under car combustible contents. In order to determine the boundary conditions at tunnel ends, a one dimensional Subway Environmental System (SES) Analysis of the tunnel network was carried out and atmospheric pressure was applied at the station entrances. Two stations were investigated, namely Pueyrredon and Medrano stations. Although the stations are  $130m$  long,  $33m$  wide and  $6m$  in height, a simple mesh of  $84.000$  elements were used due to the lack of available computational resources of the given date and the cell sizes are almost  $1m$ . Two different fire scenarios were tested and the fire was located inside the metro station for both cases. In the first scenario, fans were used to push smoke and hot gases toward the tunnel whereas the second scenario required the ventilation system to force outside air through the station exits or stairways into the station. Second fire scenario was considered to be inferior and it is suggested to operate the fans in a way that the smoke and hot gases are pushed inside the tunnel from the station. Two simulations were carried out to observe the effectiveness of the jet fan system. The jet fan capacities were determined such that the emergency requirements in the tunnel sections adjoining these stations were satisfied in SES simulations. The analysis showed that natural ventilation is not enough to prevent the buildup of hot gases at the platform and mezzanine areas during a station fire and it is impossible to maintain acceptable conditions for evacuating passengers without sufficient mechanical ventilation. The simulations showed that for a fire inside the station, operating the jet fan system would draw outside air through exits or stairways into the tunnels, thus maintaining an evacuation path free of smoke and gases for passengers. For a fire at either end of the station beyond the last exit or staircase, the jet fans should be operated in the same direction to generate longitudinal airflow in the direction opposite to the evacuation path. The authors stated that natural ventilation is not sufficient to maintain a tenable environment in the station, and concluded that the jet fan system would be a cost effective solution. It is also noted that an analysis need to be carried out as a future work to compare the CFD performance with available experiments such as Memorial Tunnel Test. In 2001, NIST researcher Kevin McGrattan [19] investigated the fire incident in Howard Street Tunnel, Baltimore which occurred by

the derailment of 11 car train. A tripropylene tank was ruptured and the spilled fuel was ignited causing the catastrophic fire inside a 2.5km long tunnel which burned for several days. The same scenario with the same geometry, boundary conditions and fire source was modeled in Fire Dynamics Simulator. The derailed cars were located inside the tunnel based on the reports prepared after the accident. The researcher used numerical cells with sizes ranging from 15cm to 30cm near the fire source and a coarse mesh was used far away from the fire. The tunnel walls were modeled as brick with a known specific heat and thermal conductivity. The aim of the study was to estimate the maximum temperature and heat flux inside the tunnel. The size of the fire was determined as 50MW by making detailed calculations which is basically driven by the amount of fuel present inside the fuel tank. It was decided that the fire was oxygen limited, and it could reach to higher heat release rates if more oxygen were present. As a result of the simulation, the author concluded that a 1000°C peak temperature was present at the fire zone and the wall temperatures reached the values of 800°C. The researcher validated his results by investigating the rail car components recovered from the train. It was noted that aluminum equipment were melted which was a proof that the temperature inside the tunnel reached above the melting temperature of aluminum which is 600°C. Later in 2005, the same researcher investigated the Caldecott fire which happened in 1982. By using FDS, and a fire heat release rate of 200MW, the maximum temperature was found as 1100°C.

In 2002, Falin Chen and Shin-Chang Guo [8] employed a CFD approach in the Gong-Guan Subway Stations of Taiwan by using a computer code named CFX4, which utilized finite volume method, in order to investigate the stack effect on smoke propagation in subway stations. The length of the station is 142m and its width is 18m. Two station levels were modeled and the height of concourse level is 4.15m, and platform level is 5.15m. The 3D model is divided into 300,000 grid elements and by using transient analysis temperature contours and velocity vectors inside the tunnel were calculated. Due to the complexity of reactions involved in fire, a source of heat and smoke were used to model the fire. All radiation effects were neglected for simplicity. A 5kW heat load and  $1.4 \times 10^5$  ppm/s of CO<sub>2</sub> is modeled along with a 10kW heat load and  $2.8 \times 10^5$  ppm/s of CO<sub>2</sub>. The  $k - \epsilon$  turbulence model was used. Constant pressure boundary condition was prescribed at the tunnel and station exits, no-slip

condition was applied at the station walls and constant velocity was prescribed at the fan inlets. Also the effect of Platform Screen Doors was investigated. Authors concluded that the evacuation system is safe and allows enough time for the passengers to evacuate. They also determined that Platform Screen Doors significantly increase the performance of smoke exhaust systems in subway stations since they prevent the movement of smoke into the station. The effect of platform screen doors can be seen in Figure 1.2.

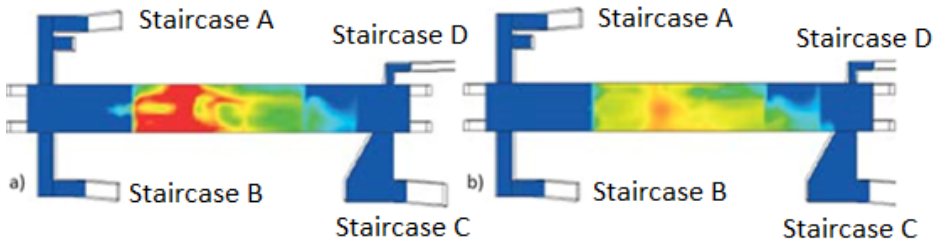


Figure 1.2: Comparison of Smoke Distributions a) without Platform Screen Door and b) with Platform Screen Door [8]

In 2005, Stephane Gaillot, Alistair Revell, and Dominique Blay [11] carried out an experimental study to verify the CFD results obtained by Fluent. Their 1 to 30 scaled down set up was based on the Paris metro system. Butane was injected and ignited in the tunnel to simulate the fire load. Walls were covered with insulation material to prevent heat transfer to the room. Researchers investigated the critical velocity by observing the back layer formation at different velocities. They used Laser Doppler Anemometry to measure the temperature in the tunnel. Sketch of the set-up can be seen in Figure 1.3.

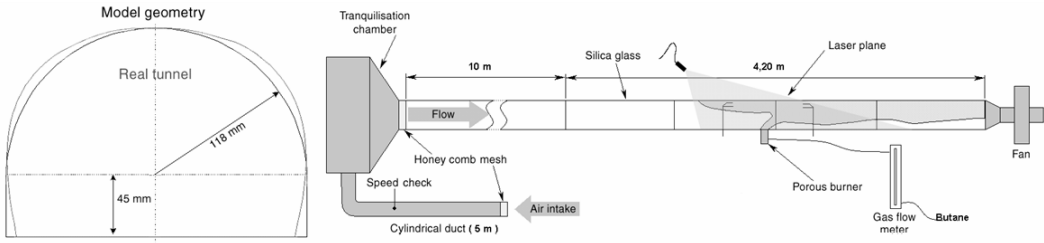


Figure 1.3: Test Set-up of Paris Metro by Stephane Gaillot [11]

The full scale geometry was modeled and meshed by using the Gambit software.

CFD solution was carried out by FLUENT 5.4. The radiation effects were ignored and the fire was modeled as a heat generating volume composed of a cube. Symmetry boundary conditions were utilized at the median plane in order to save computational time. Tunnel walls were defined as adiabatic since the test set-up was well insulated. Velocity inlet was defined for the tunnel inlet and a mass flow rate equal to that of the inlet was defined for the tunnel exit plane, which is arguable due to the contribution of plume to the flow rate in the experimental setup. The authors obtained plots of back-layer length versus Richardson number from both experimental and computational data and saw that the results are in a reasonable agreement. Authors concluded that the small differences between the numerical and experimental studies are due to the effect of wall heat transfer and radiation effects.

Serkan Kayılı [14] carried out simulations using CFDesign 7.0 in order to determine the safest evacuation scenario. The steady state and transient analyses were performed with the three dimensional geometry of two different subways namely KCK and Polytechnica Metro Stations. Both transient and steady state solutions were obtained and the solutions were compared with the Fire Dynamics Simulator results. The fire was represented as a source of smoke and heat. During the transient simulations, the fire was modeled by using the  $t^2$  approximation where fire heat release rate is growing with the square of time and the simulation was carried out for 6 minutes. The fans are assumed to start 30 seconds after the beginning of the simulation. The results of the simulations are given as contour plots of velocity, temperature and smoke concentration distributions. The author concluded that FDS gives almost the same results as CFDesign 7.0 and they can be used interchangeably for fire safety studies. As a result of the simulations, it is concluded that the KCK Station scenario is able to keep the station temperature and visibility within the required limits of NFPA 130. For the Polytechnico Station, it is observed that temperatures go above  $60^{\circ}\text{C}$  and the situation might get worse for fires at different locations. Therefore, it is suggested to include additional fans at the stations or install separate jet-fans at the evacuation routes which will direct the smoke to the exhaust fans and keep a tenable environment at the station exits.

In 2007, Serkan Kayılı and Cahit Eralp [16] studied a fire simulation case in an Istanbul Metro Station. The station length is  $125\text{m}$ , width is  $21\text{m}$ , and the height is  $6.17\text{m}$ .

They carried out a steady state simulation of 15MW train fire by using CFDesign 9.0. They used a full scale model and a mesh of 800,000 elements. No slip boundary conditions and no heat transfer conditions (adiabatic) were applied at the walls, and the boundary conditions at the two ends of the tunnel were determined by carrying out a 1D SES simulation. Two exhaust fans are located at each end of the station and each fan has a flow rate of  $100m^3/s$ . The train body was modeled as aluminum. By using  $k - \epsilon$  turbulence model, modeling the fire as a source of heat and smoke, and taking the ambient temperature to be  $330^\circ C$ , they obtained plots of smoke density and velocity. They concluded that the evacuation routes are clear of smoke and the temperatures are below  $50^\circ C$  throughout the escape routes.

In 2007, Jae Seong Roh et.al [24] carried out simulations in a metro station by making use of Fire Dynamics Simulator. A 10 car train is located at the station which is 220m long, 15m high and 24m wide. It is assumed that the fans start operation 60s after the start of the fire and Over Track Exhaust fans have a total capacity of  $50m^3/s$ . Simulations are carried out for cases with and without platform screen doors, and ventilation. LES turbulence model, mixture fraction model, finite volume method of radiation transport for a non-scattering grey gas, and conjugate heat transfer between wall and smoke flow are used in FDS simulation. The heat release rate is assumed to reach 35 MW in 5 minutes which corresponds to an fire growth factor of  $385W/s^2$  which is based on an experiment carried out in 1994. Mesh independency study is carried out by checking the time required for smoke to reach a reference plane. 1,000,000 cells are used as an optimum value along with refined meshes close to the fire. Atmospheric boundary conditions are applied at the tunnel ends and station entrances, and the fuel used is composed of polyethylene, polypropylene, nylon, polyester and polyurethane which resulted in a smoke yield of  $0.08kg/kg$ . The visibility and temperature contours along the escape routes at a height of 1.8m were plotted. Another simulation with the platform screen doors were carried out and the two simulations were compared. The authors conclude that the platform screen doors contribute significantly in maintaining a tenable environment since they guide the smoke to the over track exhaust duct and prevent the smoke to propagate into the metro station.

In 2011, Manabu Tsukahara and Yusuke Koshiba [29] investigated the Daegu Station fire which took the lives of 192 people. By creating a 3D model of the 3 floors

of the station and dividing the domain into 52,000 cells, with nominal cell sizes of  $x = 120\text{cm}$ ,  $y = 122\text{cm}$ ,  $z = 101\text{cm}$ , they carried out calculations on Fire Dynamics Simulator. Six train cars, each with  $18\text{m}$  length were modeled. Hexane was used as the fuel and smoke density, temperature and concentrations of  $CO$  and  $CO_2$  were investigated at staircases for 10 minutes. The heat generation rate was taken as  $1\text{W}/\text{m}^2$  at the outer surface of the train and the fire was modeled to be growing based on the scenario that happened in the Daegu subway station. Smoke generation rate was  $21\text{m}^3/\text{min}$  for 7 minutes with an increment of  $66\text{m}^3/\text{min}$  for every minute after 7 minutes. The authors concluded that all the escape routes were covered with smoke after 4 minutes and the fire fighters could not enter the station. Second analysis was done with a 4<sup>th</sup> floor in the station which is below the platform level. Authors suggested to use this floor for evacuation purposes and showed that the floor underneath the platform (B4) stays smoke free throughout the whole simulation. They came up with an innovative solution to the problem by suggesting an under platform floor to be used for emergency evacuation purposes. Moreover, the under platform level can also be used for the access of firefighters since it is seen to be free of smoke at all times. It is also advised that passengers in B1 and B2 levels should evacuate the station by the staircases since they are unaffected from the fire for the first 3 minutes. The smoke distribution inside the four floors of the station for four minutes can be seen in Figure 1.4.

In 2011 Alper Çelik [32] created a pool fire by using ethanol and gasoline in the Fluid Mechanics Laboratory of the Mechanical Engineering Department at the Middle East Technical University Laboratories. He also carried out simulations on FDS to compare his experimental results such as heat generation and mass loss rate at different velocities. He created a 1/6 scaled down model of the Istanbul Metro Tunnel. His test set up can be seen in Figure 1.5.

Experiments were carried out by using  $100\text{ml}$ ,  $200\text{ml}$ ,  $300\text{ml}$  gasoline pools under  $0.5\text{m}/\text{s}$ ,  $1.5\text{m}/\text{s}$  and  $2.5\text{m}/\text{s}$  tunnel ventilation velocities. A fan was used to obtain different air velocities and separate tests were carried out for each different velocity value. The mass loss rate was measured by making use of a digital balance whereas the air velocity was measured by a Pitot tube. The pool fires were carried out by using square and rectangular pools and the results were compared with the available

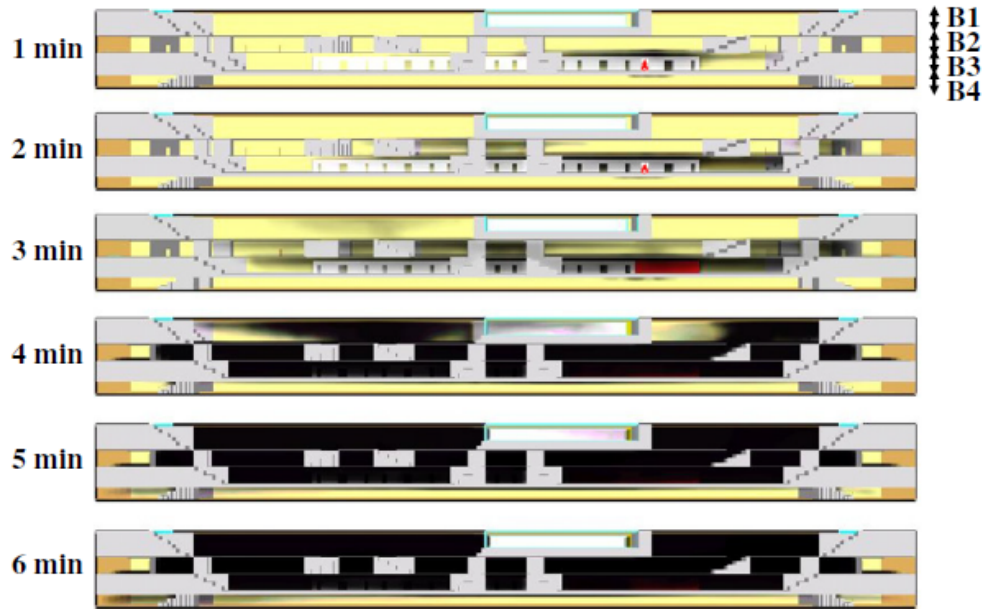


Figure 1.4: Smoke behavior in all 4 levels of Daegu Metro Station for 6 minutes [29]



Figure 1.5: Pool fire set-up of Alper Çelik [32]

research. The author concluded that the fire is fuel controlled, and the change in air velocity does not affect the heat release rate very much, whereas the increase of fuel mass increases the heat release rate drastically. 100ml, 200ml and 300ml ethanol pool fire was simulated on Fire Dynamics Simulator and the results showed that the heat release rate values and mass loss rate values calculated by FDS overshoots the

experimental data. The author draws attention to the fact that FDS does not perform very well in the case of estimating the heat release rate from pool fires.

In 2011, Wang Binbin [6] investigated the Tianjin Xiawafang subway station in China, and compared FDS results, Fluent results and experimental results in order to assess the accuracy of two CFD software. The 5 to 1 scaled experiment was carried out in Tianjin Xiawafang station and it is known as the largest station test ever carried out. The author applied widely used standard  $k - \epsilon$  two equation turbulence model in Fluent and used LES method for FDS simulations. The platform length is modeled as 120m and the same geometry and the same number of cells were used in the two different softwares. The heat release rate of fire was set to a constant value of 5MW, and it was initiated at the middle of middle compartment. The simulation was carried out for six minutes and contour plots were obtained at the end of each minute. Gasoline was used as the fuel of combustion. The author states that Fluent has more advantages such as different methods of mesh generation, different turbulence models, ability to handle curved structures, therefore it is able to solve more complex flow problems. However, when temperature,  $CO_2$  concentration and smoke layer thicknesses were compared with experimental results the author concludes that although FDS gives more accurate estimations. In almost all measured parameters such as  $CO_2$  concentration, temperature, smoke layer thickness, it is observed that FDS results are closer to the experimental values.

In 2014, Bouzid Benkoussas, Amor Bouhdjar, Olivier Vauquelin [5], carried out their simulations in a relatively small station in Algeria. The length of the station is 70m, width is 14m and the height is 4m. The domain was divided into cells of 25cm. The train is composed of 4 cars with lengths of 16m and the heat release rate is considered to be constant as 15MW. The smoke extract fans at both ends of the station each have a flow rate of  $50m^3/s$  and atmospheric boundary conditions at the staircases. The tunnel entrance conditions were investigated as (1) no ventilation through tunnels (NVT); (2) total air exhausted through tunnels is less than the amount supplied by the station supply fans (LVT); (3) total air exhausted through tunnels is equal to the amount supplied by the station supply fans (MVT) and (4) total air exhausted through tunnels is higher than the amount supplied by the station supply fans (HVT). The temperature plots were obtained along the center plane which is 1.5 m above

the floor level. Also plots showing the smoke fields were obtained for each different scenario. It is observed that for different fire locations most of the simulations prevailed satisfactory results however the least successful ventilation strategy is “HVT”, when the total flow rate through the tunnels is about 30% higher than that extracted flowrate. Since there is excess air pumped into the station, the smoke particles tend to stay in the station and excess fresh air is taken through the station fans. The situation gets worse as the flow rate coming from the tunnel is increased. Therefore the authors conclude that if the smoke is being extracted from the stations, the amount of fresh air supplied to the tunnel should be below the extracted flowrate. This would allow some air to be taken from the staircases and create safer path for the passengers.

In 2016, Yan Fu Wang et al. [30] carried out full scale train fire tests in tunnel, and compared the results with the CFD simulations carried out on Fluent Software by using  $k - \epsilon$  model. The tests were carried out in a 1.5km tunnel with height of 5.75m and width of 12.35m. A 7.5MW fire was created by burning diesel oil and temperature was measured at various locations by the use of 48 copper thermocouples and velocity was measured by traversing the cross section with an anemometer. One fifth of the tunnel length is modeled in the Fluent simulation, and a mesh independent study was carried out by checking the drag coefficient of the train. The authors decided to use the grid number of 425,000 since the solution only differs by 1% when compared to a grid with one million cells. Alpha  $t^2$  approach is applied in order to simulate the fire growth period. In this approach, the fire heat release rate is assumed to grow with the square root of time. The outlet boundaries are given the pressure outlet conditions, and the walls are assumed to be at 7°C throughout the simulation. The fire growth factor is taken as  $47W/s^2$ . The simulation results and full scale experimental results were compared by the measurements of temperature at different locations. All the simulation results agree well with the experimental data, and as a result, it is seen that the tunnel ceiling temperature is kept below 110°C. The author concludes that this cost effective CFD model can be used instead of carrying out full scale experimental tests on tunnel fires.

One of the latest tunnel fire studies was carried out in 2017 by Andrew Purchase et al. [23] where different factors affecting the evacuation in the metro tunnels such as the ventilation, tunnel area, walkway depth and the slope in the tunnel were investigating

by making use of FDS software. The researchers investigated a mid-train fire with the train located inside the tunnel which is determined to be the worst case scenario for tunnel fires. Researchers computed the values of visibility, temperature, and  $CO_2$  concentration and by making use of appropriate correlations, they calculated the Fractional Incapacitating Dose (FID). This value was used to compare the safety levels of each different fire scenario. The authors concluded that increasing the tunnel area and the walkway width has a significant contribution to the tunnel safety. However there is no conclusion about the effect of tunnel ventilation in case of a mid-tunnel fire since the results differ for different simulations. Authors also noted that temperature and smoke concentration are lower on the trackway compared to the elevated walkways, therefore evacuation from the trackway can be carried out in a safer manner.

A validation study was carried out by Steve Cochard [10] in 2003, by simulating a 40MW fire and comparing the obtained values with the readily available experimental data of Memorial Test Program. The exact parameters used during the Memorial Test was used including the tunnel geometry, tunnel lining materials and heat release rate and boundary conditions. The author obtained continuous temperature measurements from 56 different points in FDS and compared these values with the measured results of Memorial Test Program. As seen in Figure 1.6, most of the results are within 15%.

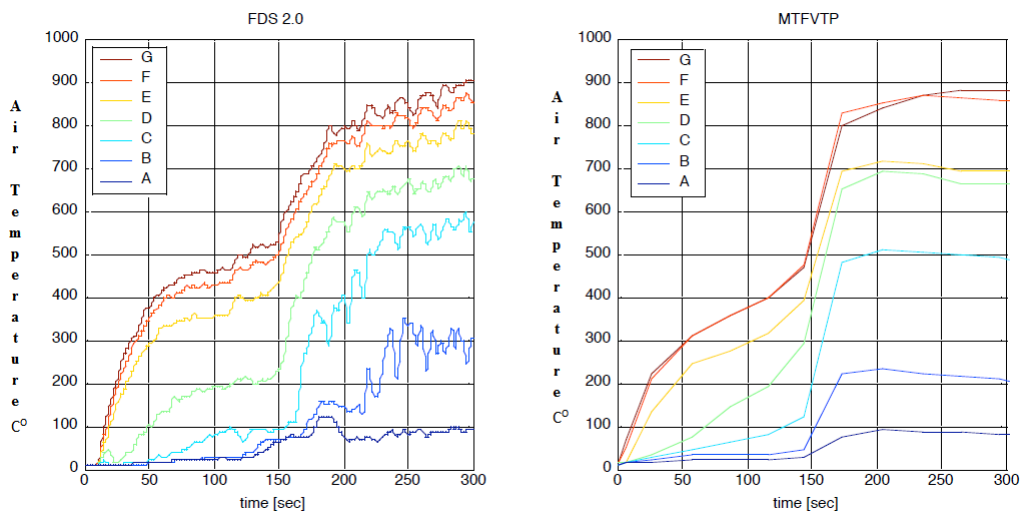


Figure 1.6: Comparison of FDS Data with Experimental Data [10]

When compared with the experimental results, it is also noted that the simulation

overestimates the temperatures before the ventilation is started and it underestimates the temperatures once the ventilation is running at full speed. The author concluded that the overall performance of FDS is acceptable and FDS code can be used with confidence for fire analysis.

In 2015, Uluc Yamali [31] carried out experiments on 1/13 scaled tunnel of Istanbul Metro to investigate the effect of ventilation velocity, pool depth and pan geometry on pool fires in tunnels. He used pools of ethanol and n-heptane, and made use of Oxygen Consumption Calorimetry to compute the Heat Release Rate of the fire. A total 27 thermocouples were located at different locations of the tunnel and values were recorded throughout the experiment. A fan with variable speed is used to set the air velocity inside the tunnel to values between  $0.5\text{m/s}$  and  $2.5\text{m/s}$ . He concluded that heat release rate depends strictly on ventilation velocity and reaches the maximum value at  $1\text{m/s}$  ventilation velocity. To see the effect of radiation, interior surfaces of the tunnel was covered with a reflective material for some experiments and it was concluded that ratios of convective heat to radiative heat transfer is 55% under  $1\text{ m/s}$  and it is 25% under  $2.5\text{m/s}$ .

## **1.5 Full Scale Tunnel Fire Tests**

Large scale testing is extremely expensive and time consuming to carry out, but it is essential to understand the tunnel fire phenomena and validate the CFD results. The first test was carried out in 1965 to compare different ventilation modes such as longitudinal, natural, semi-transverse in the Ofenegg Road Tunnel. After 1970's, the use of oxygen consumption calorimetry made it possible to measure the Heat Release Rate accurately. Table 1.1 shows the previous fire tests carried out inside the tunnels with budgets ranging from hundreds of thousand dollars to millions of dollars:

## **1.6 Tunnel Ventilation Concept**

Ventilation systems in tunnels are being used for over a hundred years. The early applications were installed to cope with contaminants produced by vehicles like diesel

Table 1.1: Full Scale Tunnel Tests

Location and Date	Fire Source	Measured Data	Heat Release Rate (MW)
Ofenegg, Switzerland, 1965	Gasoline Pool	Temperature, $CO$ , $CO_2$ , visibility, velocity	11-80
Glasgow, 1970	Kerosene Pool	Temperature, Optical Density	2-8
Zwenberg, Austria, 1974	Gasoline Pool, Wood and Rubber	Temperature, $CO$ , $CO_2$ , velocity, $O_2$ , $NO_x$	8-21
Japan, 1980	Gasoline Pool	Temperature, $CO$ , $CO_2$ , velocity, Optical Density, radiation	9-14
Finland, 1985	Wood Cribs	Heat Release Rate, Temperature, Mass loss rate, $CO$ , $CO_2$ , $O_2$ , velocity, Optical Density	1.8-8
EUREKA, Norway, 1990-1992	Wood, heptane pool, cars, metro car, etc.	Heat Release Rate, Mass loss rate, Temperature, $CO$ , $CO_2$ , velocity, $O_2$ , visibility, soot	2-120
Memorial, USA, 1993-1995	Fuel Oil	Heat Release Rate, Temperature, $CO$ , $CO_2$ , visibility, velocity	10-100
Simizu, Japan, 2001	9m <sup>2</sup> Gasoline Pool	Temperature, velocity, Optical Density, radiation	2-30
The Netherlands, 2002	Heptane, toluene, car, van and HGV	Heat Release Rate, Temperature, Mass loss rate, radiation, velocity, Optical Density, visibility	3-23
Runehamar, Norway, 2013	Cellulose, plastic, wood pallets	Heat Release Rate, Temperature, $CO$ , $CO_2$ , $O_2$ , Optical Density, radiation	70-203
Brunsbery, Sweden, 2011	Metro Car	Heat Release Rate, Temperature, $CO$ , $CO_2$ , $O_2$ , Optical Density, radiation	77
San Pedro Tunel, Spain, 2012	HGV mock up	$CO$ , $CO_2$ , $O_2$ , Optical Density, radiation	150

locomotives such as high amounts of combustion products and heat. Full transverse systems were being utilized in the early applications, in the modern applications longitudinal ventilation is preferred due to its reduced cost.

The attention on fire safety increased drastically due to accidents that occurred in the past few decades and many regulations have been built to cope with the problem of tunnel fires.

During a fire, tunnels cannot be compartmentalized like standard buildings, therefore firefighters have to fight the fire within the fire zone. Limited access creates difficulties with suppressing the fire. Therefore, tunnels require a detailed analysis of emergency ventilation.

There are two different modes of ventilation systems; namely Longitudinal Ventilation System and Transverse Ventilation System.

### **1.6.1 Longitudinal Ventilation**

In longitudinal ventilation, the airflow is longitudinal through the tunnel and essentially moves the polluted air along with the incoming fresh air and extracts it from the other end of the tunnel. This can be achieved by using either jet fans inside the tunnel, or tunnel ventilation fans at the entering or exiting portal. Longitudinal Ventilation is preferred in most of the modern tunnel applications including all rail projects of Istanbul. This type of ventilation can be from portal to portal, shaft to shaft, or portal to shaft. The descriptions are depicted in Figure 1.7:

### **1.6.2 Transverse Ventilation**

Transverse flow is created by the uniform distribution of fresh air and/or uniform suction of pollutants along the length of the tunnel. The uniformity of the airflow throughout the tunnel is helpful to maintain similar conditions within the tunnel. [4] This is achieved by placing many vents positioned along the tunnel for supply and exhaust as seen in Figure 1.8:

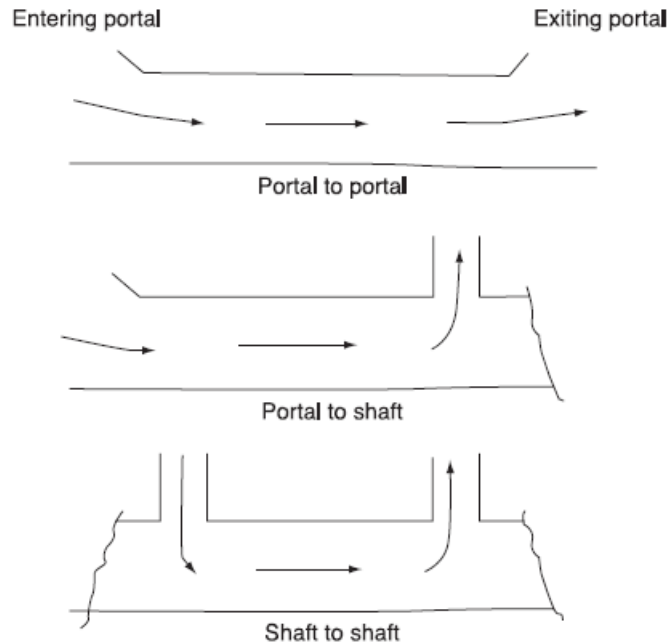


Figure 1.7: Longitudinal Ventilation

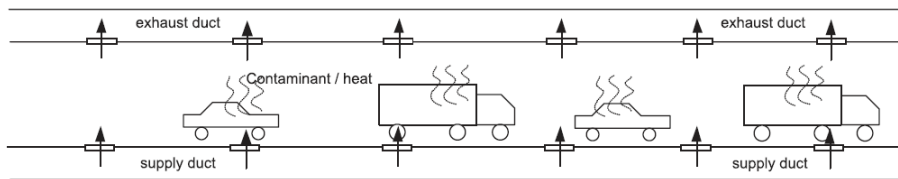


Figure 1.8: Transverse Ventilation

The main difficulty with transverse ventilation is the need of additional area to install the supply/exhaust ducting which increases the cost in tunneling projects.

Longitudinal ventilation is the commonly used method in tunnels and for fire safety, since it is very expensive to apply transverse ventilation systems in underground metro stations due to the extra cross-sectional area needed for ventilation.

Longitudinal ventilation system should be operated in such a way that if the fire is in the front train car, ventilation should direct the smoke to the direction of train movement to keep the passengers free of smoke. If the fire is in the rear of the train, the smoke is directed towards the back of the train to keep the passengers free of smoke given that the non-incident train behind the incident train is taken to the safe zone so that passengers on the rear train will not be affected by smoke. Figure 1.9 explains how passengers are evacuated during a fire at the end of the train.

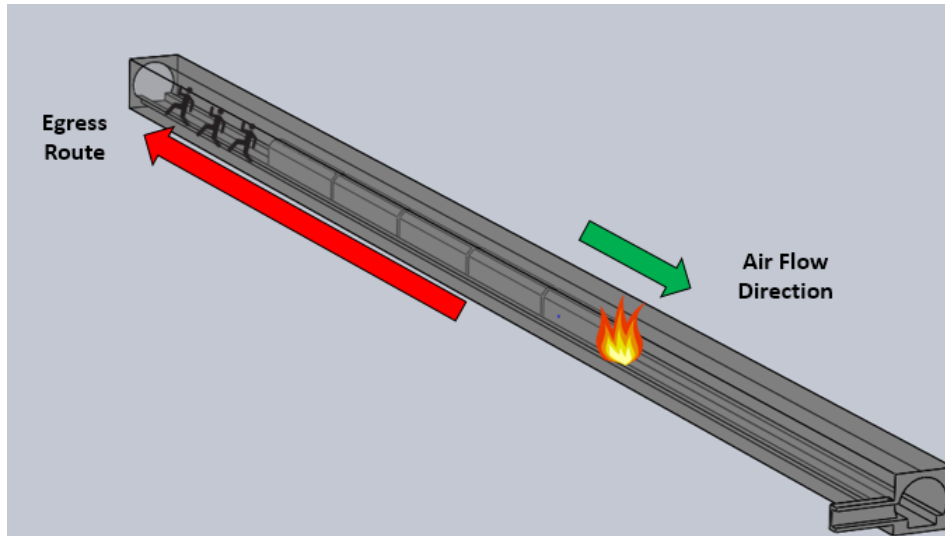


Figure 1.9: Egress Route in Tunnel Fire in Case of a Fire at End Location

The most problematic situation is when the fire is at the middle of the train, thus it is impossible to create smoke-free path for all the passengers in each ventilation mode. If the ventilation system is activated, half of the passengers will be effected by smoke and hot gasses, and if the ventilation system is not activated all of the passengers might be effected of smoke and hot gasses before they can self-evacuate. Therefore, detailed analysis is required for fires that are in the middle of the train and this thesis focuses on specifically the fire case on the middle of the train.

### 1.6.3 Critical Velocity in the Tunnel

In the event of a fire in a tunnel without ventilation, hot combustion products rise to the ceiling and create two smoke streams flowing symmetrically in two longitudinal directions of the tunnel. If a ventilation system is installed, the symmetry is broken by the flow of air and the smoke and hot gasses are directed towards the downstream direction. This is crucial in creating an evacuation path for the passengers. Back-layering occurs when the upper layer of heated air and smoke flows in the opposite direction of tunnel ventilation. This may happen if the ventilation is weak, i.e. the flow velocity is lower than the critical velocity.

During an emergency case the velocity inside the tunnel should be greater than the critical velocity in order to prevent reverse flow of smoke from a fire inside the tun-

nel. This parameter (critical velocity) is the first step in designing tunnel ventilation systems and the design velocity should be greater than this value in order to prevent backlayering. It gives the order of magnitude for tunnel velocity in case of a fire. The critical velocity is calculated by solving the following equations simultaneously [2]:

$$V_c = K_1 K_g \left( \frac{gHQ}{\rho c_p A T_f} \right) \quad (1.1)$$

$$T_f = \frac{Q}{\rho c_p A V_c} + T \quad (1.2)$$

$$K_g = 1 + 0.0374(gr)^{0.8} \quad (1.3)$$

where,  $V_c$  is the critical velocity ( $m/s$ ),  $T_f$  is the average temperature of fire site gasses( $K$ ),  $K_1$  is 0.606,  $K_g$  is Grade Factor  $g$  is acceleration caused by gravity ( $m/s^2$ ),  $H$  is height of duct or tunnel at fire site ( $m$ ),  $Q$  is heat that fire adds directly to air at fire site ( $kW$ ),  $\rho$  is density of approaching air ( $kg/m^3$ ),  $c_p$  is specific heat of air ( $kJ/kg \cdot K$ ),  $A$  is Area perpendicular to flow ( $m^2$ ) and  $T$  is Temperature of approaching air ( $K$ ).

During the design of the system, the maximum velocity has to be limited so that people can walk safely in the tunnel. According to NFPA 130, [3] air velocities above  $11.0m/s$  can threaten the evacuation and this value should never be exceeded throughout the evacuation.

#### 1.6.4 Critical Velocity in the Cross Passage

The main purpose of the tunnel ventilation system is to keep the evacuation routes clear of smoke in case of a fire. In a fire scenario the passengers are expected to escape through the nearest cross passages to the non-incident tunnel. Therefore, the cross passages need to be free of smoke until all the passengers are evacuated. Cross passages are also strategic locations that allow firefighters to access the fire zone. Figure 1.10 shows the cross section view of a cross passage and tunnel in a well ventilated fire scenario: The ventilation system has to be designed such that the cross passage is kept clear of smoke. This is possible by pressurizing the non-incident tunnel and creating an airflow from the non-incident tunnel to the incident tunnel. The velocity inside the cross passage have to be greater than the critical value in

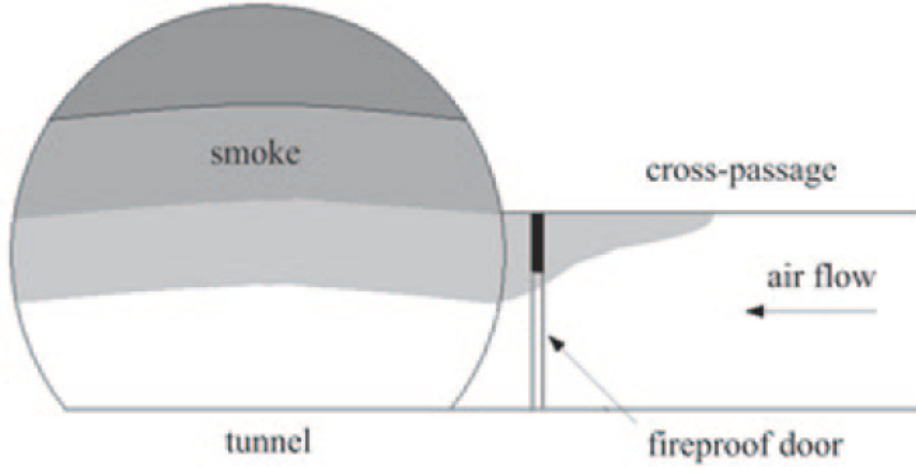


Figure 1.10: Typical smoke distribution in a tunnel with cross passage [12]

order to keep the evacuation path free of smoke. The critical velocity for a cross passage can be calculated by using the following formula:

$$v_{cc}^* = 1.65(H_c^*)(Q_t^*)^{(1/3)}e^{-v_t^*} \quad (1.4)$$

$$v_{cc}^* = \frac{v_c}{\sqrt{gH_c}} \quad (1.5)$$

$$H_c^* = \frac{H_c}{H_t} \quad (1.6)$$

$$Q_t^* = \frac{\dot{Q}}{\rho_0 c_p T_0 g^{1/2} H_t^{5/2}} \quad (1.7)$$

$$v_t^* = \frac{v_t}{\sqrt{gH_t}} \quad (1.8)$$

where  $v_c$  and  $v_t$  are the cross passage and tunnel velocities,  $H_c$  and  $H_t$  are the cross passage and tunnel heights. The velocity inside the cross passage is designed to be greater than  $v_c$  in order to prevent the smoke from entering the cross passage.

## 1.7 Tenable Environment for Humans

Tenable environment is the environment that supports human life for a specific period of time. This needs to be examined in underground metro stations in order to assess the safety of the emergency routes which is the main purpose of fire safety systems. Fire produces high temperatures, heat radiation, low concentration of oxygen, low

Table 1.2: Exposure Time to High Temperatures

<b>Exposure Temperature</b>	<b>Maximum Exposure Time</b>
80°C	3.8 min
70°C	6.0 min
60°C	10.1 min
50°C	18.8 min
40°C	40.2 min

visibility and toxic gasses which seriously threaten the survival of passengers and the duration of tenability limit should be calculated with reasonable accuracy.

Thermal burns to the respiratory tract can occur upon inhalation of air above 60°C that is saturated with water vapor which can frequently occur since water is generally used for fire extinguishing. [3] It is also noted that skin burns start occurring earlier than the respiratory tract burns and can occur at temperatures below 60°C.

Exposure to heat can cause damage in three ways, namely, through hyperthermia, body surface burns and respiratory tract burns. Tenability limit for exposure of skin to radiant and convective heat is approximated by the following formula [18]:

$$t_{exp} = (1.125 \times 10^7) T^{-3.4} \quad (1.9)$$

where  $T$  is the exposed temperature in Celsius and  $t_{exp}$  is the duration of exposure in minutes. The formula can be visualized in Table 1.2.

This empirical relationship has an uncertainty of 25% and it is used widely by many researchers in order to determine the success of fire safety systems.

In order to assess the tenability limit inside the tunnel, temperature of 60°C is taken as the maximum limit since it is a widely used maximum temperature by many other researchers.

Visibility is also an important parameter since ability to follow the evacuation path is a factor of how well the evacuees can see the surroundings. According to NFPA 130, [3] people inside the station should be able to see the surface of walls from a distance of 10m and they should be able to see luminous exit signs from a distance of 30m in order to evacuate the fire scene safely. This criterion is applicable for metro stations, where large open areas are present and distance of the walls are greater considered to

tunnels. However, for the case inside the tunnel where the maximum distance of each passenger to the wall is less than  $3.5m$ , the visibility criterion can be reduced to be  $5m$  as explained by Alan Beard and Richard Carvel [4].

In order to assess the tenability limit in the tunnel, the minimum acceptable visibility is taken as  $5m$  and it is assumed that evacuation of people will not be affected significantly given that the visibility is above  $5m$ .

It is important to determine the time needed to evacuate the tunnel in order to assess the tenability criteria and see if the escape routes are clear throughout this evacuation period. Assuming that the Marmaray 5 car train is full, 1637 passengers need to evacuate the tunnel by either through the station or the cross passage located downstream of the fire. Since the fire is located at the middle of the train, it is assumed that half of the passengers will evacuate through the cross passage and will be subject to smoke and high temperatures whereas the other half will be at the upstream side of the fire and reach safety through the station given that backlayering is not present.

The person at the last train car needs to walk a distance of  $80m$  in order to reach the closest cross passage and given that the minimum egress travel speed is  $1m/s$  as found in experimental studies of Miho Seike et. al. [26] It can be said that the first passenger will reach the cross passage within 80 seconds after the detection of fire.

Every cross passage door has a net width of  $1930mm$  and according to NFPA 130, for doors and gates the constant of  $0.0893\text{people}/mm - \text{min}$  should be used to determine the evacuation time. Assuming that the train is at full load and 819 people will evacuate through the cross passage, it can be said that passengers will take 285 seconds to cross the door.

By adding these two values, evacuation time of all the passengers can be calculated as 365 seconds. Therefore, the tunnel needs to be kept at the explained tenable conditions for 365 seconds after the detection of the fire. It is further assumed that people with disabilities will be assisted by commuters to help them reach the cross passage within the evacuation time.

## 1.8 Description of Marmaray Tunnel

Marmaray is the Metro Line that connects the European and Asian sides of Istanbul, the World's 6<sup>th</sup> most populated city. 1.387 meters of the tunnel is under the water and the deepest part is 60m below the sea level. The metro line is composed of 5 metro stations and corresponding tunnels. Tunnels are in twin-bore, single track arrangement in other words every track is on a separately bored tunnel. Within the tunnel, cross passages are located in every 200m in order to help passengers cross from one track to the other in case of an emergency scenario. The system started operation in October 2013 and currently carries about 200,000 passengers every day.

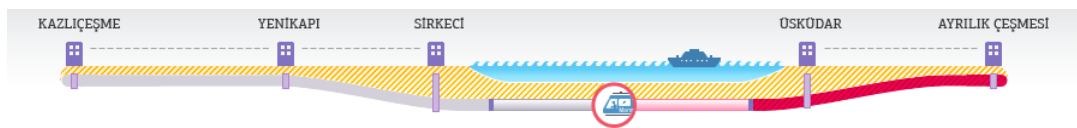


Figure 1.11: Stations of Marmaray Metro Line

The passengers are required to walk to the nearest station by using the walkways located on both sides of the track in case of a train failure in the tunnel. Therefore, smoke evacuation is crucial in this metro system since there is no escape shafts in the tunnel.

Since there are no ventilation shafts in the tunnel, the emergency ventilation is carried out from one station to the other station in a push-pull arrangement and the tunnel lengths can be up to 3.5km away from each other. A longitudinal push-pull ventilation is utilized in the fire scenarios in the tunnel sections and over track exhaust (OTE) Fans are used to clear the smoke during fire scenarios inside the stations. With the help of reversible tunnel ventilation fans (TVF) located at the two ends of the tunnel, fresh air is supplied from one station and the smoke is exhausted from the other in case of a fire scenario between the two stations. The fan operation is oriented according to the train location inside the tunnel and fire location on the train.

A 1D simulation on SES was carried out for different fire scenarios and the tunnel ventilation fans were selected to operate at a flow rate of  $144m^3/s$  with three fans are operational at each station. This study was carried out by AECOM, Tunnel Ventilation Group from USA, and the fan flow rates were verified by on-site measurements.



Figure 1.12: Marmaray Tunnel ventilation fan

Saccardo nozzles were installed at both ends of the tube, namely Yenikapı and Ayrılık Çeşmesi Stations in order to direct the flow to the required tunnel sections. The fans are fully reversible, which means that the fans can exhaust or supply air depending on the location of the fire and the train.

Smoke exhaust fans are also located inside the stations to evacuate the smoke in case of a station fire scenario. Under platform, and Over Track Exhaust fans are located in each station and their capacity is selected by making use of full scale CFD simulations in the stations. Performance of these smoke extract systems were verified by carrying out smoke tests inside each train station as seen in Figure 1.13.

At the cross-over locations where the two tunnels connect and the tunnel area increases by a factor of more than 2, Jet-Fans are utilized to direct the smoke towards the extract direction. Without the Jet-Fans it is not possible to reach the critical velocity in this area due to the drastic increase of tunnel area.

There are two tunnels each occupied with a single track, and the height of the tunnel is 6.2 meters. The cross section area of each tunnel is  $33.26m^2$ .

The passenger train is designed and manufactured by the Korean company Hyundai Rotem with the body material of stainless steel. Each rolling stock is composed of 5 cars, and each car is 22.5m long. Height of a train car is 3.80m and the width is 3.01m.



Figure 1.13: Smoke Test in Sirkeci Metro Station

The maximum heat release rate of one train car in case of a fire is given as  $20MW$  by the manufacturer and the emergency ventilation system is designed by making use of this value.



Figure 1.14: Marmaray Train

The 5 car train is capable carrying 1637 passengers with 248 people sitting and 1389 people standing.

## CHAPTER 2

### MODELING OF FIRE

In order to model the fire scenario by using CFD, Navier Stokes Equations are solved numerically. The most important characteristic of different CFD models are the ways that they handle the turbulence terms. Turbulence modeling is difficult to predict in flow simulations, and the complexity is a lot more for the cases with fire and smoke spread. There are three commonly applied methods, namely Direct Numerical Simulation (DNS), Reynolds Averaged Navier Stokes (RANS) and Large Eddy Simulation (LES). Among these three, DNS directly accounts for turbulent terms, whereas LES ignores the smallest length scales by low-pass filtering, and RANS model ignores the turbulent fluctuations and aims to calculate only turbulent averaged flow. In large scale CFD problems, DNS is very difficult to apply since it directly accounts for turbulent terms and requires very small computational domains.

In order to solve the conservation equations by DNS, the grid resolution must be smaller than Kolmogorov scale which is the length scale of the smallest turbulent eddies( $\eta$ ).

$$\eta \equiv \left(\frac{\nu^3}{\varepsilon}\right)^{1/4} \quad (2.1)$$

Here  $\nu$  represents kinematic viscosity and  $\varepsilon$  is the rate of viscous dissipation which is defined by:

$$\varepsilon \equiv \tau_{ij} \frac{\partial u_i}{\partial x_j} = 2\mu \left( \frac{1}{2} \left( \frac{\partial u_i}{\partial x_j} + \frac{\partial u_j}{\partial x_i} \right) - \frac{1}{3} (\nabla \cdot u)^2 \right) \quad (2.2)$$

Resulting Kolmogorov length scale for typical fires is in the order of one millimeter. Therefore, it is very difficult to model fires by using Direct Numerical Simulation. DNS approach is feasible in cases where Reynolds number is low, and the geometry is very simple.

LES requires less computational time compared to DNS, but it is more difficult to solve compared to RANS. LES can predict more detailed results whereas RANS gives average results and lacks the ability to deliver detailed solutions. Therefore, LES is generally preferred to model flows including fire and smoke spread.

Large Eddy Simulation approach makes use of low pass filtering in order to ignore the smallest scales associated with high frequencies. Large eddies are retained and solved for directly using transient calculation. Therefore, the equations of mass, momentum and energy conservation cannot be used directly but must be simplified so that they can be efficiently solved.

The Navier Stokes equations are filtered and a computationally more effective solution is obtained by sacrificing a small amount of accuracy. The low pass filter is given in the below equation.

$$\bar{\Phi}(x, y, z) = \frac{1}{V_c} \int_{x-\frac{\Delta x}{2}}^{x+\frac{\Delta x}{2}} \int_{y-\frac{\Delta y}{2}}^{y+\frac{\Delta y}{2}} \int_{z-\frac{\Delta z}{2}}^{z+\frac{\Delta z}{2}} \Phi(x', y', z') \quad (2.3)$$

Fire Dynamics Simulator (FDS) is one of the most popular tools used by fire safety engineers and it makes use of LES approach to solve the Navier Stokes Equations.

## 2.1 Fire Dynamics Simulator

Fire Dynamics Simulator (FDS) is a CFD based software which is developed by Building and Fire Research Laboratory which is a branch of NIST (National Institute of Standards and Technology) and released in 2000, and 6 versions have been released since that date.

The software is written in Fortran language and it is aimed to solve practical fire problems in fire protection engineering, and provide a tool to study fundamental fire dynamics and combustion. Smokeview is an accompanying software which helps to visualize and interpret the outputs of the FDS. Both softwares are open source and available for all researchers.

Mass, momentum and energy conservation equations are solved using finite volumes and the solution is updated in time on a 3D rectilinear grid. Thermal radiation is mod-

eled by finite volume method using the same grid. Smoke movement and sprinkler effect are modeled by making use of Lagrangian particles. The solution outputs can be visualized in the form of contour plots or graphs as in any commercial CFD software. More detailed information about the software and governing equations can be found in FDS Technical Guide. [20]

Fire Dynamics Simulator consists of the following components:

**Geometry:** FDS solves the equations on rectilinear grids. The user defines the geometry by using rectangular blocks.

**Boundary Conditions:** All surfaces are assigned thermal boundary conditions and/or information about the burning characteristic of the material. Heat and mass transfer from solid surfaces is computed by empirical correlations.

**Hydrodynamic Model:** FDS solves a form of Navier-Stokes equations for low-speed, thermally driven flows with an emphasis on smoke and heat transport from fires. Turbulence is modeled by the LES method.

**Combustion Model:** FDS uses a combustion model based on mixing and infinitely fast reaction of lumped species. Lumped species are reacting scalar quantities that represent a mixture of species.

**Radiation Transport:** Radiation is accounted in the simulations by the solution of radiation transport equation for a grey gas. The radiation equation is solved by using finite volume method. The absorption and scattering coefficients are based on the Mie theory. The scattering from the gaseous species and soot is not included in the model.

### 2.1.1 Combustion Modeling Using Mixture Fraction

Modeling combustion is extremely difficult due to the necessity of extreme levels spatial and temporal resolution. In general, the flame thickness is on the order of millimeters, the eddies caused by introduction of air into the fire are in the order of centimeters and the flow field generated by a fire inside the tunnel is in the order of meters. Therefore, it is too expensive to construct a grid fine enough to resolve the flame sheets except for cases where the domain is small. Moreover, the actual chem-

ical processes that control the combustion are often unknown in fire scenarios due to partial burning of fuels in multistep reactions. Even if they were known, the temporal and spatial resolution required to directly model a combustion is computationally very expensive.

Therefore, some simplifications have to be utilized in order to successfully model combustion. The simplest method is to represent the fire zone with volumetric heat flux, thus avoid the complexity that comes with modeling of combustion process with some sacrifice of accuracy.

To increase the accuracy and get more realistic results, the mixture fraction method is used in FDS. Mixture fraction method assumes an infinitely fast, single step reaction. This method traces the fractions of fuel and oxygen to find flame sheet location. Heptane is used as the source of fuel since it is a generic hydrocarbon fuel and its properties are pre-defined in Fire Dynamics Simulator.

Mixture fraction combustion model is based on the assumption that large scale convective and radiative transport phenomena can be simulated directly, but physical processes occurring at small length and time scales must be represented approximately. By making use of mixture fraction approach, the transport equations for major gas species are combined into a single equation for a conserved scalar known as mixture fraction  $Z(x,t)$ . Therefore, all species of interest can be described in terms of a mixture fraction, which represents the fraction of material at a given point that is in the fuel system. This quantity is defined as the fraction of the fluid mass that originates as fuel. From this quantity, mass fractions for all other species can be derived based on semiempirical state relationships. By using the state relation for the oxygen mass fraction, local oxygen mass consumption rate is obtained. The form of state relation that emerges from classical laminar diffusion flame theory is a piecewise linear function as seen in Figure 2.1.

It can be clearly seen that  $Z$  varies from 1 in a region of only fuel to 0 the region of only air. This leads to a “flame sheet model” where the flame is a two dimensional surface in a three dimensional space. By making use of the local oxygen consumption at the flame surface, local heat release rate is calculated. This assumes that the heat release rate is independent of fuel involved and it is directly proportional to the

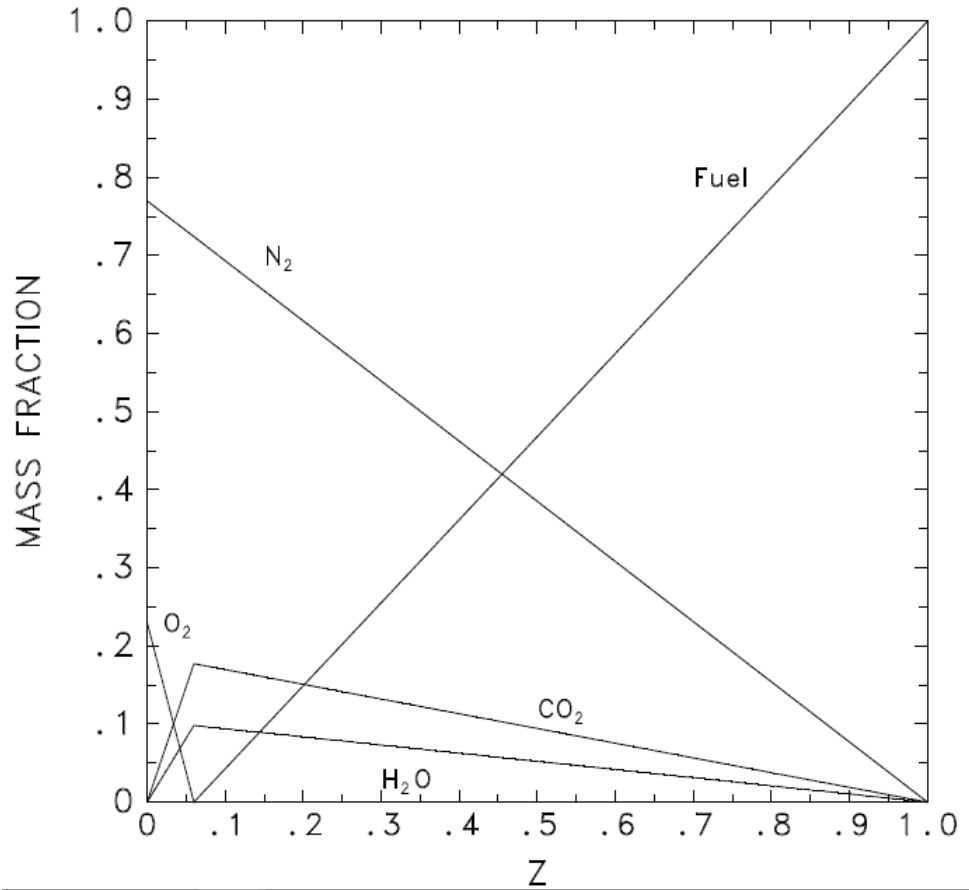
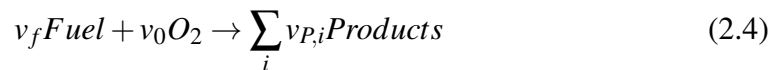


Figure 2.1: State Relations for Propane

oxygen consumption rate which is the basis of oxygen calorimetry.

One simple method to couple the combustion process with the flow field is to track three species; fuel, nitrogen and oxygen. Since convective processes are much longer compared to combustion processes, it can be assumed that reaction occurs infinitely fast. This method requires the solution of three species and in order to simplify this, it should be noted that both fuel and oxygen cannot be present together in an infinite rate reaction. The most general form of combustion can be written as



$v_i$  values are the stoichiometric coefficients of the reacting species. By using the above relationship, the mass consumption rates for fuel and oxidizer can be related as

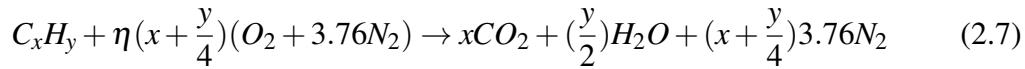
$$\frac{\dot{m}_F'''}{v_F M_F} = \frac{\dot{m}_O'''}{v_O M_O} \quad (2.5)$$

where  $M_F$  and  $M_O$  are molecular weights ( $kg/mol$ ) of fuel and oxygen. By using this relation, the mixture fraction  $Z$  is defined as:

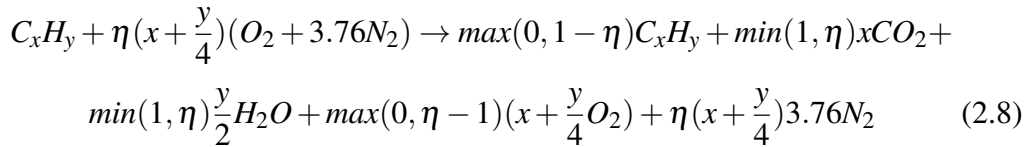
$$Z = \frac{sY_F - (Y_O - Y_O^\infty)}{sY_F^I + Y_O^\infty}; s = \frac{v_O M_O}{v_F M_F} \quad (2.6)$$

where  $Y_O^\infty$  defines the ambient oxygen mass fraction and  $Y_F^I$  is the fraction of fuel in the fuel stream.

State relations for both reactants and products can be derived by considering the following ideal burning reaction of a typical hydrocarbon fuel:



In a real case combustion, the ideal equation above will not be present due to the stoichiometric conditions since either fuel or oxygen will be in excess. The reaction for the real case is shown in the following equation



Here  $\eta$  is a multiplier to account for the relative amounts of fuel and oxygen and it is ranging from 0 (only fuel and no oxygen) to infinity (only oxygen with no fuel).  $\eta$  and  $Z$  can be related by applying definition of  $Z$  given by Equation 2.6 to the left hand side of the above equation. However, since the mixture fraction assumes infinitely fast chemistry, what is present in the computational domain is the right hand side of the above equation. Therefore, in the computational domain only the products are present.

By using Equation 2.6, the mass fractions of products in Equation 2.8 can be plotted as a function of  $Z$ , as seen in Figure 2.1. The flame sheet is defined to exist at the point where both fuel and oxygen disappear from the products. The mixture fraction corresponding this point is designated as  $Z_F$  and this point is the exact point where the reaction is represented by Equation 2.7, i.e. there is no excess oxygen or excess fuel at this point. If the  $Z$  values in the domain are larger than this value, that means excess fuel is present and if the  $Z$  values in the domain are smaller than this value, that means excess oxygen is present.

In order to use the mixture fraction in the computation, an expression for the local heat release rate as a function of mixture fraction is needed to be utilized. The heat release rate can be computed by using oxygen calorimetry and assuming that local oxygen consumption is directly related to the heat release rate. The following two transport equations are written for the conservative terms mixture fraction and oxygen mass fraction, respectively:

$$\rho \frac{DZ}{Dt} = \nabla \cdot \rho D \nabla Z \quad (2.9)$$

$$\rho \frac{DY_{O_2}}{Dt} = \nabla \cdot \rho D \nabla Y_{O_2} + \dot{m}'''_{O_2} \quad (2.10)$$

The two equations can be multiplied by  $dY_{O_2}/dZ$  and subtracted from each other, to yield:

$$-\dot{m}'''_{O_2} = \nabla \cdot \left( \rho D \frac{dY_{O_2}}{dZ} \nabla Z \right) - \frac{dY_{O_2}}{dZ} \nabla \cdot \rho D \nabla Z \quad (2.11)$$

It can be seen in Figure 2.1, that  $dY_{O_2}/dZ$  is constant on one side of the flame sheet and zero on the other. The volume integral can be rewritten as surface integral over the flame sheet by applying Gauss's divergence theorem.  $dY_{O_2}/dZ$  is either zero or a constant depending on which side of  $Z_F$ , the computed zone is.

Since  $dY_{O_2}/dZ$  term will be 0 in this region and  $Z > Z_F$ , this region can be ignored. The result is the mass loss rate of oxygen as a function of the mixture fraction diffusion across the flame surface, which is given as:

$$-\dot{m}''_{O_2} = \left. \frac{dY_{O_2}}{dZ} \right|_{Z < Z_F} \rho D \nabla Z \cdot n \quad (2.12)$$

Since oxygen is a function of only the mixture fraction, this is equal to saying that global heat release rate is a function of oxygen gradient across the flame sheet. This equation states that the heat release rate is solely due to the diffusion of oxygen across the flame which is already given by the hydrodynamic solver.

### 2.1.1.1 Radiation Modeling Equations

Radiation has an important role in fire scenarios due to the high difference of temperature between the fire source and surrounding surfaces. It is also a complex problem

since there are contributions from many species like soot,  $CO_2$  and  $H_2O$ . The radiation process is characterized by absorption, emission and scattering of radiant energy.

The spectral intensity radiation,  $I_\lambda(\hat{r}, \hat{s}, \hat{t})$ , at wavelength  $\lambda$  is found from the radiative transport equation which describes the addition of absorption, emission and scattering. Radiation transport equation for absorbing/emitting and scattering equation is:

$$s \cdot \nabla I_\lambda(x, s) = -[\kappa(x, \lambda) + \sigma_s(x, \lambda)]I(x, s) + B(x, \lambda) + \frac{\sigma_s(x, \lambda)}{4\pi} \int_{4\pi} \phi(s, s') I_\lambda(x, s') d\Omega' \quad (2.13)$$

where  $I_\lambda(x, s)$  is the radiation intensity at wavelength  $\lambda$ ,  $s$  is the direction vector of the intensity  $\kappa(x, \lambda)$  and  $\sigma_s(x, \lambda)$  are the local absorption and scattering coefficients, respectively, and  $B(x, \lambda)$  is the emission source term. The integral on the right hand side describes the in-scattering from other directions. In the case of a non-scattering gas, the radiation transport equation becomes:

$$s \cdot \nabla I_\lambda(x, s) = \kappa(x, \lambda) [I_b(x) - I_\lambda(x, s)] \quad (2.14)$$

where  $I_b$  is defined as the source term given by Planck function. This section describes the radiation transport in the gas phase.

In practical simulations, the spectral dependence cannot be solved accurately. Instead, the radiation spectrum is divided into a relatively small number of bands, and separate Reynolds transport equation is derived for each band. The limits of the bands are selected to give an accurate representation of the most important radiation bands of  $CO_2$  and water. The Reynolds transport equations for  $N$  number of bands are as follows:

$$s \cdot \nabla I_n(x, s) = \kappa_n(x) [I_{b,n}(x) - I_n(x, s)], n = 1, 2, 3, \dots, N \quad (2.15)$$

where  $I_n$  is the intensity integrated over the band  $n$  and  $\kappa_n$  is the appropriate mean absorption coefficient inside the band. The source term can be written as a fraction of the blackbody radiation as

$$I_{b,n} = F_n(\lambda_{min}, \lambda_{max}) \sigma T^4 / \pi \quad (2.16)$$

where  $\sigma$  is the Stephan Boltzman constant. The calculation of factors  $F_n$  is given in Siegel and Howell [25]. When the intensities corresponding to the bands are known,

the total intensity is calculated by summing over all the bands.

$$I_{x,s} = \sum_{n=1}^N I_n(x,s) \quad (2.17)$$

From a series of numerical experiments, it has been found that addition of six bands are usually sufficient. If the absorption of fuel is known to be important, separate bands can be included for fuel and total number of bands is increased to ten.

### 2.1.2 Limitations and Assumptions

Although FDS can handle most physical fire involved problems, the software has some limitations:

**Low Speed Flow Assumption:** The software is accurate for Mach numbers below 0.3. Therefore, it is not possible to model flows with velocities approaching to speed of sound such as explosions and choked flows in nozzles. This creates no problem for the tunnel ventilation analysis since the velocities are low.

**Rectilinear Geometry:** The geometry is created by rectangular elements which makes it very difficult to model curved boundaries. The curvature of the tunnel wall is modeled by making use of small rectangular obstructions.

**Combustion:** FDS uses a mixing controlled, lumped species based combustion model. Lumped species are reacting scalar quantities that represent mixtures of gas species such as air, fuel and combustion products. The model assumes that combustion is mixing controlled and the reaction between oxygen and fuel occurs immediately. This is a good assumption for well vented, large space fires; but introduces errors for under-ventilated compartment fires.

**Radiation:** Radiative heat transfer is accounted in the model by making use of grey gas assumption. First, the absorption coefficient for the smoke-laden gas is a complex function of composition and temperature. Since the model assumes a grey gas, chemical composition of smoky gasses affects the absorption and emission of thermal radiation. Second, the radiative heat transport is discretized by using 100 angles and for walls far away from the fire source, this causes hot spots where the rays hit the wall. This is called as the “ray effect”. Although this can be avoided by increasing

the number of angles, the computation time increases substantially.

### 2.1.3 Visibility

Fire safety in tunnels relies on the principle of self-evacuation which means that passengers need to be aware of their environment and evacuate the fire zone on their own. Visibility is one of the most important parameters affecting the possibilities for safe egress. Although reduced visibility in itself does not lead to incapacitation, visibility is a very critical parameter in tenability analysis.

Visibility is the distance that an observer can identify an object relative to the background. It is a very critical tenability criterion in subway analysis since it can slow down the evacuation and can cause fall injuries. It is important for passengers to have clear visibility during a fire case in order to determine the escape paths and evacuate the scene safely.

Emergency exit signs and lights are very critical for evacuation in case of emergency scenarios. Therefore, if the visibility inside the tunnel decreases, serious consequences may occur as in the case of Daegu Subway Fire in Korea where 198 people died where many victims were unable to locate the escape route.

The visibility is a complicated phenomenon and it depends on size, shape and quantity of the particles in smoke and it depends directly on the burnt material and combustion conditions. Therefore, there are many different suggestions about how to calculate visibility. The most widely used method was developed by Jin [13] and this method is also adopted in FDS.

In order to visualize the effect of smoke, and assess the visibility, a quantity called light extinction coefficient,  $K$ , is used. The smoke causes attenuation in the light and the intensity of light passing a distance  $L$  in meters through smoke is attenuated according to the following equation:

$$\frac{I}{I_0} = e^{-KL} \quad (2.18)$$

The value of light extinction coefficient is defined by the multiplication of mass specific extinction coefficient  $K_m$  ( $m^2/kg$ ) and smoke particulate as given in the below equation:

$$K = K_m \rho Y_S \quad (2.19)$$

By making use of these equations, and non-dimensional constant  $C$  which depends on the object being viewed, visibility, in meters, through smoke is defined as:

$$S = \frac{C}{K} \quad (2.20)$$

Constant  $C$  depends on the object being viewed which is determined experimentally as [9]  $C = 5$  to  $10$  for a light-emitting exit sign and  $C = 2$  to  $4$  for a reflecting sign. This value depends on the optical values of the object being viewed through the smoke. The value of  $K$  varied within the domain due to the changes in smoke particulate and density; therefore visibility changes throughout the domain and it is calculated specifically for each cell.

Smoke production and visibility in FDS is controlled strictly by the following parameters:

- Soot Yield, which is the fraction of fuel mass that is converted to soot
- Mass Extinction Coefficient is defined as  $8700 m^2/kg$  as a default value In FDS.
- Visibility Factor is set to  $3$  as default in FDS settings which corresponds to a reflecting light.

Soot yield is the driving factor that determines the visibility value in calculations and it depends on the type of the material burnt during the fire. Materials present in a typical train car is given in Table 2.1 [21].

Different materials create various amount of soot when consumed by fire. The soot yield values range from  $0.015kg/kg$  for heptane to  $0.1kg/kg$  for polyurethane. Therefore, an analysis has to be carried out to find the amount of soot that will be produced during a train fire.

In his thorough analysis, Musluoglu [21] studied a typical train car and investigated the combustion properties by analyzing different materials used in the train. In conclusion, he found out that  $0.117kg/kg$  is a good estimate of the soot yield for the

Table 2.1: Train Car Materials

<b>Component</b>	<b>Material</b>
Seat	FRP Polyester
Driving Console Assembly	FRP Polyester
Floor	Plywood
Floor covering	Styrene butadiene
Wall panel	Glass wool coated with aluminum
Window	Laminated safety glass
Bellows	WPE Vamac compound
Air-con duct	Glass wool with surface covered with aluminum sheet
Air-con materials	Fiberglass - Silicon
Door, Window Seal	EPDM 772 (Rubber)
Wiring and insulation	Different Materials
Pneumatic Brake System	Plastic, rubber

Table 2.2: Previously Used Soot Yield Values

Author	Train Type	Year	Soot Yield (kg/kg)
Jae Seong Roh Et Al.	Subway Train	2007	0.08
Eren Musluoglu	Subway Train	2009	0.117
Michael Belinsky	Passenger Train	2010	0.1
K. Kang	Subway Train	2007	0.164

investigated train car. Therefore, this value will be used during the simulations in this thesis. In Table 2.2, soot yield values used by other researchers are given:

#### 2.1.4 Validation of Fire Dynamics Simulation in Literature

Before using a modeling software, it is important to determine how well the mathematical model predicts the actual physical phenomena of interest. This is mainly done by comparing the model predictions with the experimental measurements. Many scientists carried out tests to validate the results obtained by FDS on many different industrial applications.

A scaled tunnel fire experiment is used in order to validate the results of this study and it is explained in Chapter 5. This section summarizes the previous validation studies from the literature.

Steve Cochard [10] carried out FDS simulations of a 40MW fire and compared his results with the memorial tunnel experiment as explained in Section 1.4 and he validated the accuracy of the calculated temperature data.

The most thorough research was carried out by U.S. Nuclear Regulatory Commission [22] where they carried out 6 sets of large scale experiments including heptane pool fires in halls, plywood fire in rooms, ethanol pool fires with 100kW to 4MW heat release rates. All set ups are equipped with meshes of thermocouples to investigate the results. Validation was carried out for the following items:

**Hot Gas Layer Temperature:** Average values of hot gas layer temperatures were compared with the simulation results and it is observed that predicted results are within the measurement uncertainties with a few exceptions where the temperature

is over predicted.

**Ceiling Jet Temperature:** The ceiling temperatures tend to be over predicted slightly by the FDS model, but it is noted that the results are within the measurement uncertainties.

**Flame Height:** It is difficult to measure the flame height precisely, therefore the height is estimated by making use of the photos taken during the experiment. It is seen that FDS can predict the height in well-ventilated fires but they over-estimate the flame height in some measurements.

**Plume Temperature:** The temperature in the plume is difficult to predict due to the mixing of the hot gasses and combustion products. It is observed that FDS over predicts the plume temperature in some cases, but remains within measurement uncertainties for other cases. The over-estimation is related to the over-estimation of the flame height. Therefore, the users are warned to approach with caution during simulations that involve plume temperature.

**Oxygen and Carbon Dioxide Concentration:** In most of the tests, FDS can accurately estimate the gas concentrations for well-ventilated combustions with known stoichiometric values.

**Smoke Concentration:** Smoke density predicted by FDS is compared with the measurements and it is seen that FDS over-predicts the smoke concentration. Measurement tolerance is 33% but some predictions have errors of 60%.

**Compartment Pressure:** The measured pressure values are compared with the predicted FDS results and the data seems to be in good correlation with the measured values. All predicted results are within the experimental uncertainties.

**Radiation, Total Heat Flux and Target Temperature:** The surface temperature and heat flux is compared with the measured data and it is observed that FDS predicts fairly in surfaces with simple geometries. It is also observed that if the surface is close to the fire source, FDS tends to make over estimations.

It is concluded that for a fire which the heat release rate is known, FDS can reliably predict gas temperatures, major gas species concentrations, and compartment

pressures to within 15% accuracy, and heat fluxes and surface temperatures to within 25% accuracy.



## CHAPTER 3

### SITE MEASUREMENTS

Subway Environmental Systems (SES) is a widely used 1-D CFD software developed for underground transportation systems. During design stage of Istanbul Metro, analyses were carried out by the designers of the Marmaray Tunnel Ventilation System for different fire scenarios in the tunnel. Tunnel ventilation fans and over track exhaust fans were selected according to the calculated critical velocities as a result of the SES analysis.

The equipment and systems were installed in accordance to the design values. It is very important to check if the system is operating according to the design values during commissioning of the tunnel ventilation system. In order to verify the design values, on site cold flow tests were carried out inside the tunnels for various different fire scenarios. The results obtained from the onsite measurements were then used as boundary conditions in Fire Dynamics Simulator for this thesis.

During the cold flow tests, the velocity at the tunnel and cross passage is measured and these values are used as boundary conditions for the Fire Dynamics Simulator in order to assess the safety of the tunnel in case of a fire.

#### **3.1 Tunnel Velocity Measurement**

By making use of the SES software, the flow rates at different locations inside the tunnel and stations are calculated by the system designers. In order to conclude that tunnel will be safe in the event of a fire incident, site measurements are carried out and compared with these design values. To do this, air velocity is measured inside

the tunnel and flow rate is calculated by multiplying the measured velocity with the cross-sectional area.

To measure the air velocity, alternative measurement tools such as vane anemometer, hot wire anemometer and Pitot tube are available. Since the cross sectional area is large, and velocity fluctuations occur across the measurement plane, a grid system that covers the entire tunnel cross-section have to be utilized and measurements need to be taken simultaneously.

The grid system was designed with reference to ASHRAE Fundamentals 2013, Chapter 36 [1] on Measurement and Instruments. To account for the effect of wall friction and the decrease of velocity near the tunnel walls, the log-Tchebycheff ( $\log - T$ ) method was adopted, and the locations of the measurement points were selected accordingly. Five diameters have been chosen with six locations on each circle positioned every  $60^\circ$  as seen in Figure 3.1. This arrangement allowed a measurement grid of 30 points. Pitot tubes were manufactured in accordance with the Figure 3.1.

A steel platform with wheels (test rig) was constructed in order to mount the pitot tubes, which are each  $3m$  long. The heavy platform gave the rigidity to resist the vibrations from the oncoming flow.

The tubes were connected to the test rig by nuts and bolts. The rigid platform was moved to the test location with the help of track wheels mounted. Brake pads were also installed to stop the test rig after it is positioned at the correct location. The total and static pressure was measured by separate tubes mounted back to back as seen in Figure 3.2.

The data acquisition system composed of 6 wireless pressure transducers which transferred the differential pressure data to  $4 - 20mA$  signal and transferred the measured data to the TESTO computer software at every 20 seconds. The current values in  $mA$  were then converted back to pressure values in Pa with the help of the software. A different pressure value was obtained for each the 6 Pitot tubes and average velocity was calculated by making use of Bernoulli's Equation.

The train is also positioned at the test location in order to account for the extra resistance inside the tunnel which is already accounted for in SES Simulations carried

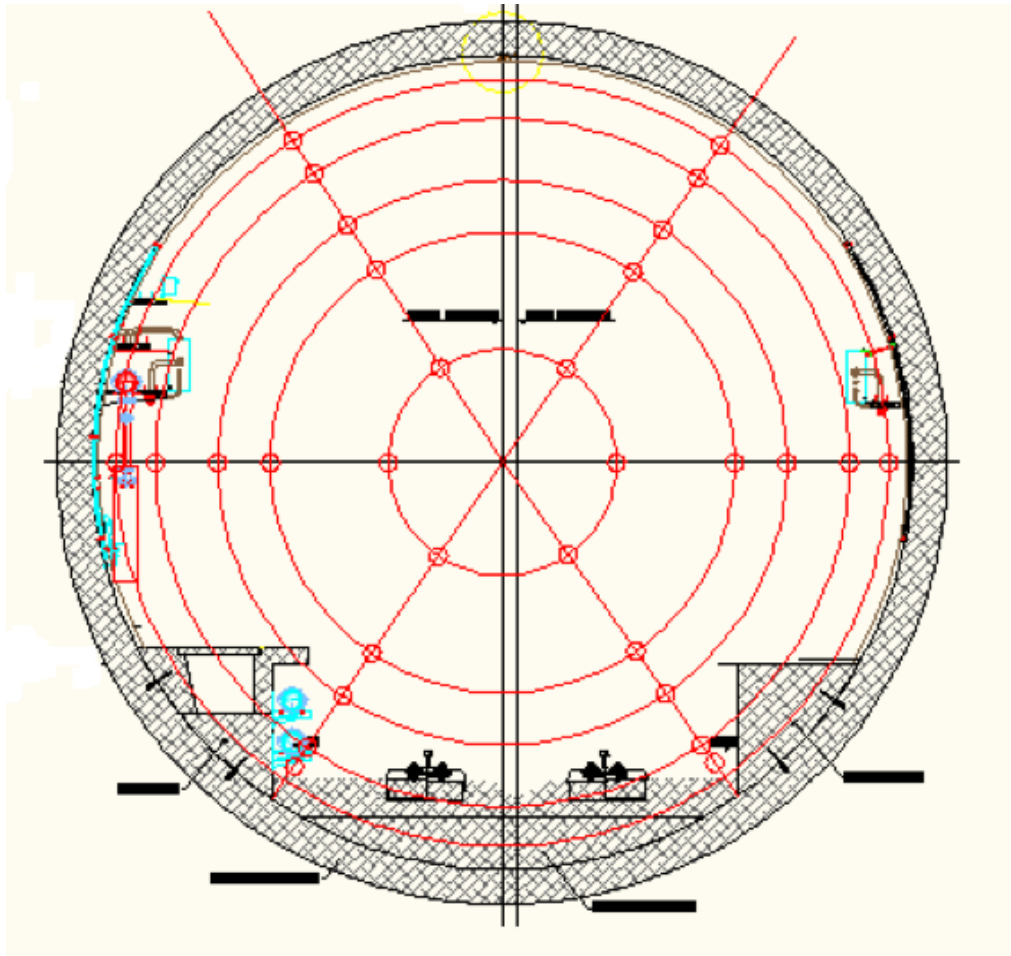


Figure 3.1: Measurement locations on tunnel cross-section for 30 point layout

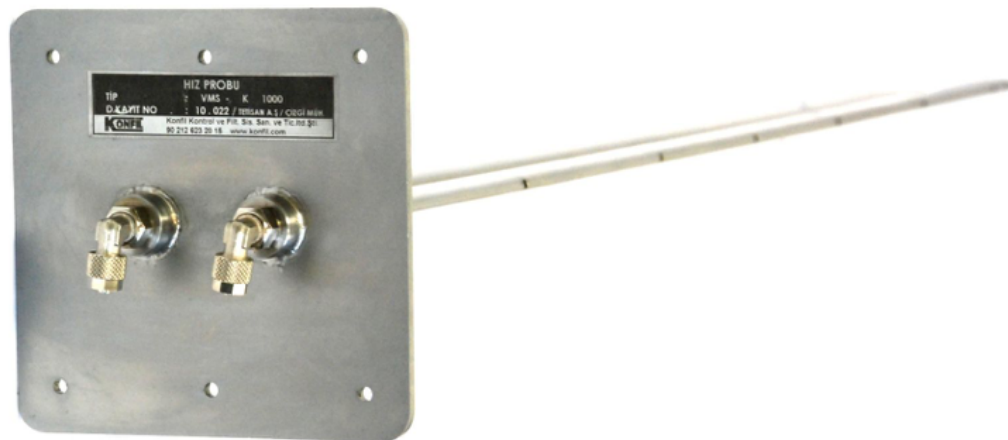


Figure 3.2: Total and static pressure tubes

out by tunnel ventilation system designers. In order to avoid the disturbance in the airflow caused by the presence of the train, measurement was carried out at a specific distance from the train. ASHRAE Fundamentals [1] states that “Measuring points should be located at least 7.5 hydraulic diameters downstream and 3 hydraulic diameters upstream from a disturbance (e.g. caused by a turn or blockage etc.)”. Since the tunnel diameter is  $7m$ , the test set up is positioned  $25m$  upstream of the train.

The differential pressure readings from the Pitot tubes were collected with six differential pressure transmitters (Dwyer 610 series low differential pressure transmitter) and transferred to PC unit using the Testo software. By using the simplified form of Bernoulli’s equation velocity values were calculated.

$$P_t - P_s = \frac{\rho v^2}{2} \quad (3.1)$$

In this equation  $P_t$  and  $P_s$  ( $Pa$ ) are total and static pressures measured by the Pitot tubes,  $v$  is the air velocity ( $m/s$ ) and,  $\rho$  is the density of air ( $kg/m^3$ ) which is obtained from the psychometric chart after the measurements of temperature and humidity.

The velocity values were recorded continuously and averaged to determine the air flow rate inside the tunnel. Temperature and humidity values were measured to determine the density of the air in each test. Entire test set up can be seen in Figure 3.3.

### 3.2 Cross-Passage Velocity Measurement

Cross passage velocities are crucial for fire scenarios because the safest way to escape from the tunnel fire is to reach the non-incident tunnel. If the non-incident tunnel is under positive pressure with respect to the incident tunnel, the air flows from non-incident tunnel to the incident tunnel and thus creates a smoke free environment inside the cross-passage. SES analysis also computes the flow rates inside the cross passages, and this value needs to be verified by on site measurements.

By making use of a Dwyer Series Pitot Tube and Testo 435-4 hand held digital differential pressure manometer, the velocity is measured at 25 different locations as seen



Figure 3.3: Test set-up

in Figure 3.4. The density value obtained in the tunnel velocity measurement is used as an input parameter to the Bernoulli's equation in order to calculate the velocity. The calculated velocity values are then averaged to find the average velocity and flow rate inside the cross passage.

### 3.3 Measurement Method

The following procedures are followed to obtain the average flowrate inside the tunnel:

- The test scenario, the test location (where the nose of the train is positioned), the track on which the test is being conducted, the ventilation direction, the season and the train type (passenger/cargo train) are identified.
- Safety Checklist given in Appendix A is filled out.
- The operating mode and conditions of the fan plants (number of TVF in operation, operation mode, supply or exhaust, damper positions, open or closed and fan speed) within the system is checked to ensure that fans are operating at the

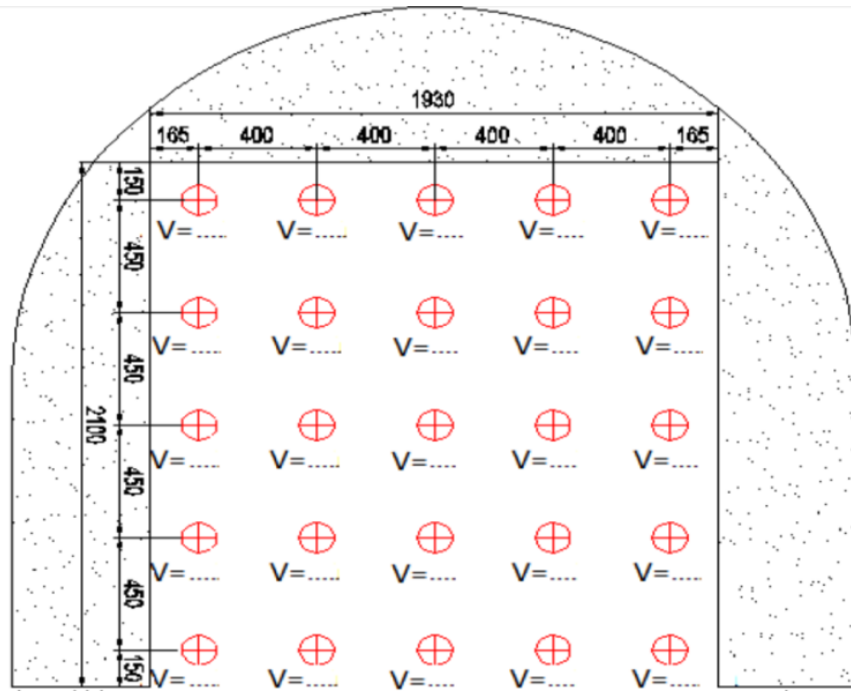


Figure 3.4: Cross passage velocity measurement

preset values specified in the applied fire scenarios.

- Air humidity and temperature are measured, and density is determined by making use of a psychometric chart.
- Tunnel velocities, measured for 15 minutes and averaged, are recorded on the test sheets. The test sheet is given in Appendix A.
- Velocities at the walkway are measured and recorded on test sheet given in Appendix A.
- Velocities at the cross passages are measured and recorded on the test sheet given in Appendix A.

### 3.4 Results of Measurements

The measurements are carried out at 7 different locations of the tunnel, with emergency ventilation system operating in each fire scenario. These locations are determined by the tunnel ventilation authorities as the most critical locations of the tunnel network.

Table 3.1: Measured Tunnel Air Velocities

<b>Emergency Scenario</b>	<b>Scenario Location</b>	<b>Design Velocity (m/s)</b>	<b>Measured Velocity (m/s)</b>	<b>% Deviation</b>
T1/4	Yedikule Station	3.51	5.11	146%
T2/4	Yenikapı-Yedikule	2.39	3.21	134%
T2/6	Yenikapı-Yedikule	3.82	4.12	108%
T4/4	Yenikapı-Sirkeci	3.41	3.44	101%
T5/4	Üsküdar-Sirkeci	3.07	2.95	96%
T7/4	Ayrılık Çeşmesi-Üsküdar	3.38	3.80	112%
T8/4	Ayrılık Çeşmesi-Üsküdar	2.30	2.59	113%

The measured volume flow rates and velocities are compared with the values computed in the SES Simulations. Different scenarios at different locations are numbered from T1/4 to T8/4.

As a result of the measurements, average velocities inside the incident tunnels were calculated for each scenario as summarized in Table 3.1.

In conclusion, the air velocity in the tunnel for emergency case is acceptable for all seven scenarios since the measured velocities are within the measurement tolerance limits or greater than the design velocities. This is deemed adequate for tunnel safety by the local authorities since the values required by the SES Simulation is verified. However, since the design is based on the 1D Subway Environmental Systems simulation, the design velocities may not be satisfactory in a real fire case where the flow is dominated by buoyancy and this situation will be investigated by making use of 3D Computational Fluid Dynamics (CFD) analysis in this study with the help of Fire Dynamics Simulator.

The section between Ayrılık Çeşmesi and Uskudar, T7/4 scenario is investigated in this study. The train is assumed to be stopped right before entering the Ayrılık Çeşmesi Station and one cross-passage door is opened for evacuation. The passengers are required to evacuate either through the cross-passage or directly through the station. The SES results can be seen in Appendix A.

Therefore, the measured air velocity of  $3.80\text{m/s}$  at the tunnel inlet is used as an input parameter to the CFD simulation. Average cross-passage velocity is measured as  $4.24\text{m/s}$  directed from the non-incident tunnel to the incident tunnel. This value is

also used as an input parameter to the simulation.

These values are greater than the critical velocity values calculated in Section 1.6.3 and 1.6.4, therefore it is very unlikely to observe back layering during the fire simulation for the given fire scenario. In order to clearly see the effect of ventilation in case of a train fire, first scenario will be carried with fan operation starting 120 seconds after ignition, and the second scenario will be carried out without fan operation.

## CHAPTER 4

### SIMULATION

Fire Dynamics Simulator is used in this thesis due to its reliability and widespread use in fire involved scenarios. The software is specifically developed for fire applications.

The geometry, in this thesis, is composed of a 5 car train and a tunnel. It was assumed that the train stopped inside the tunnel at the station entrance and the fire was initiated at the middle of the third train car since the mid-train fire is the most critical case in terms of tunnel ventilation. Although trains are programmed to stop at stations in emergency situations, it is not rare to see passengers using emergency brakes and causing the trains to stop inside the tunnel such as the case with the Zurich Metro Fire [7]. The fire in this study is located at the bottom of the middle car and it is assumed to be growing with time up to the value of  $20MW$ . The boundary conditions are obtained from on-site measurements as explained in Chapter 3 and applied to the simulation. The scenario set up is explained in the following sections.

Two sets of simulations are studied in this thesis and results are compared. The only difference between the two simulations is that in the first simulation tunnel ventilation fans are activated at  $120^{th}$  second whereas the fans are not activated throughout the simulation in the second case.

#### 4.1 Geometry

The geometry is composed of the train and the tunnel and it is modeled in SolidWorks 2015 software and imported to Fire Dynamics Simulator. The curved structures such as the tunnel roof were modeled as small rectangular pieces since FDS supports only

rectangular geometries.

In order to investigate the smoke spread clearly, a computational domain of  $250m$  is used in the simulation.  $45m$  of tunnel upstream of the train is also modeled in order to account for the hydrodynamic entry length of the air inside the tunnel. The tracks and wheels are not modeled, since they will have a small effect on the accuracy of the solutions, but they will increase the computational time significantly. Only one cross passage is modeled in the geometry since the other doors are far away from the incident location, and their doors will remain closed.

The tunnel geometry is created by making use of small rectangular elements. The height of the tunnel is  $6.2m$ . The walkways are present on the right and left side of the tunnel and they are located  $1.15m$  above the floor of the tunnel which corresponds to the  $y = 1.9m$ . For simplicity details like firehose cabinets, electrical trays, drainage pipes and tracks are not modeled since they do not contribute significantly to the simulation results. The tunnel area is  $33.06m^2$ .

One cross passage is modeled and it is assumed that the passengers will be evacuating the tunnel through this cross passage. The location of the cross passage is  $80m$  from the end of the train and the cross passage area is  $4m^2$  with a height of  $2.10m$  and width of  $1.93m$ . The cross-section view of the tunnel can be seen in Figure 4.1.

The train modeled is Hyundai Rotem which is currently being used in Istanbul Metro Lines. The width of the train is  $3m$ , the height is  $4.4m$  and the length of each train car is  $22.5m$ . The entire train geometry is composed of 5 cars which add up to a total of  $112.5m$ . Complicated geometry features such as windows, doors, and wheels are not model since they will not have a significant effect on the temperature and velocity distribution inside the tunnel. The train area is  $22.26m^2$  and the train is immobilized inside the tunnel. The air movement inside the train is of small interest and does not have a very important contribution to the temperature distribution at the walkways and therefore entire train is modeled as a solid object with adiabatic boundary conditions.

Specific damage to the train cars such as broken windows or collapsed compartments were not included in the simulations. Throughout the study, the train dimensions remained the same, since it is difficult to predict such behaviour.

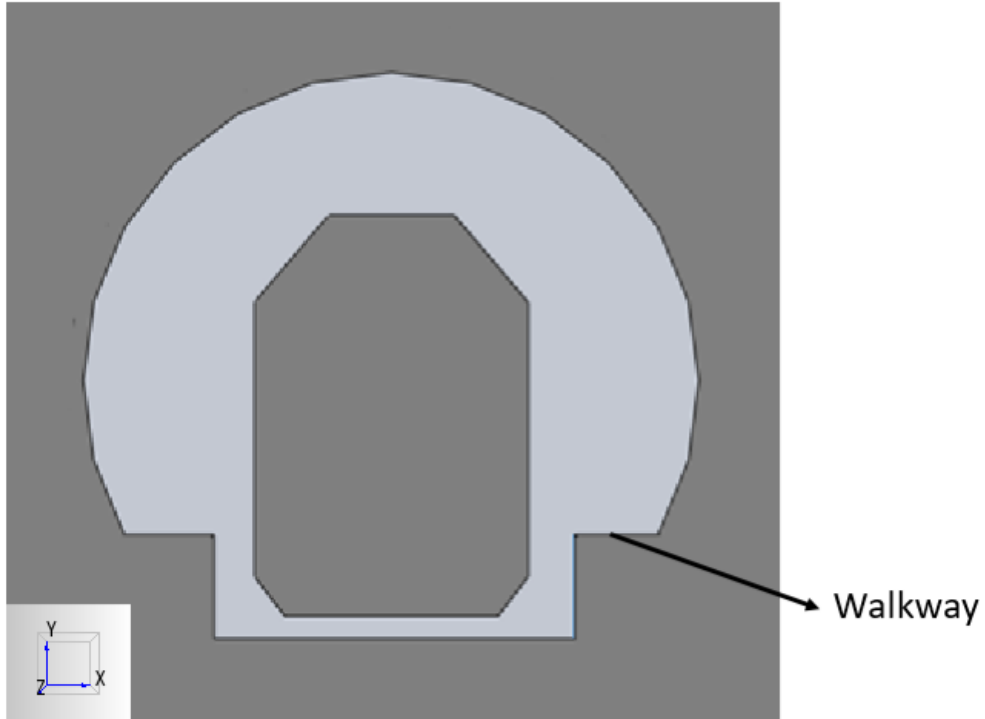


Figure 4.1: Tunnel Cross Section

The full scale 3D model of the train and tunnel can be seen in Figure 4.2.

#### 4.1.1 Meshing

FDS allows for use of only rectangular meshes defined in three dimensional coordinates  $x$ ,  $y$  and  $z$ .

When using CFD, it should be noted that finer meshes generate better results, however the computational time increases as the mesh is refined. The quality of mesh in FDS is defined by the non-dimensional ratio of  $D^*/\delta x$  which is the ratio of characteristic fire diameter to the cell size. The quality of the mesh increases as this ratio increases. Previous FDS validation studies show that a ratio of 5 to 10 produces favorable results at a moderate computational cost [22].

Fire characteristic diameter  $D^*$ , can be calculated by the following formula:

$$D^* = \left( \frac{\dot{Q}}{\rho_{\infty} c_p T_{\infty} \sqrt{g}} \right)^{2/3} \quad (4.1)$$

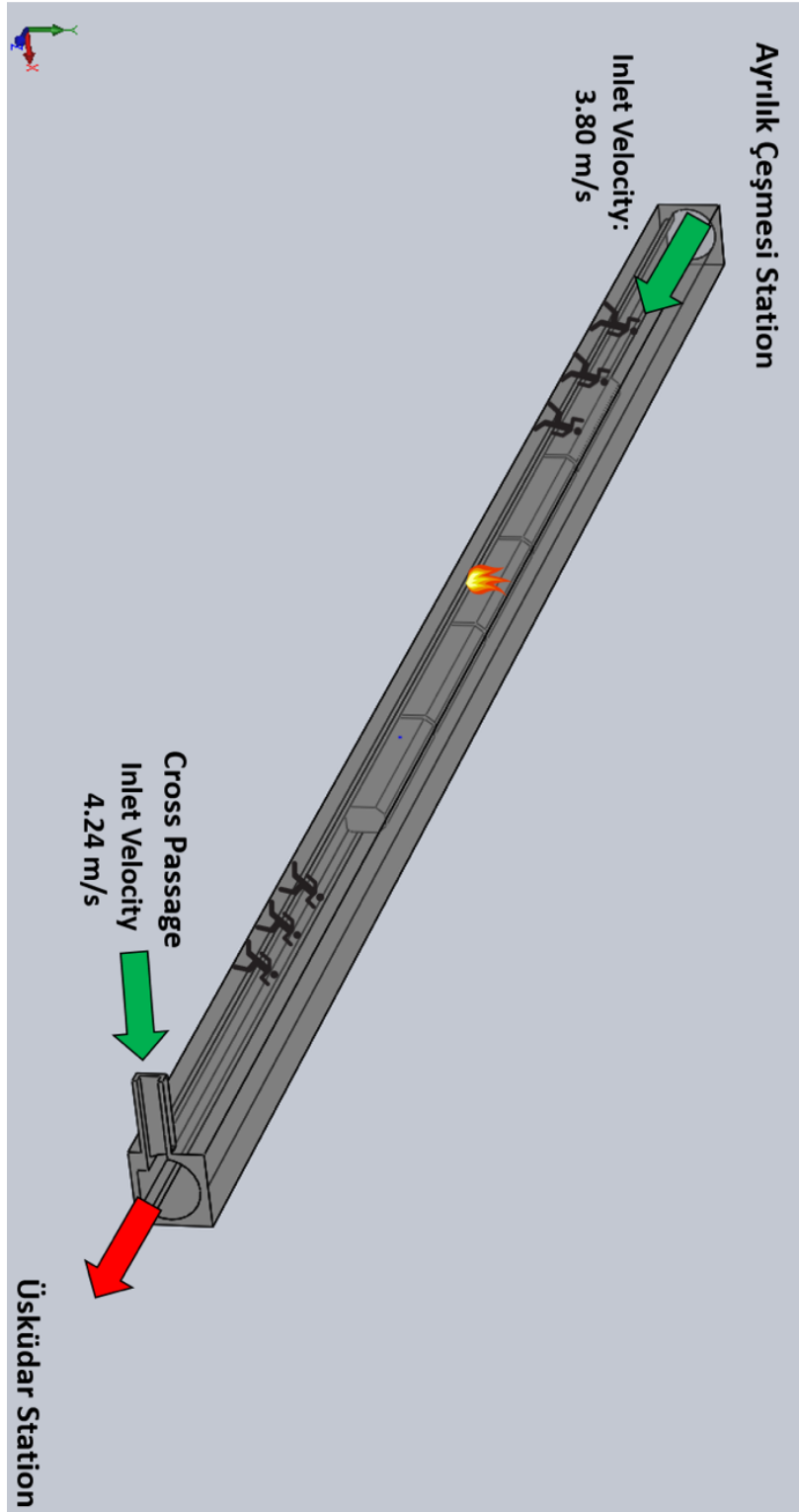


Figure 4.2: CAD Model of Tunnel and Train

The computational domain is discretized in 369.311 cells with nominal cell sizes of  $x = 0.35\text{cm}$ ,  $y = 0.35\text{cm}$ ,  $z = 0.35\text{cm}$ .

For a 20MW fire and cell size of 0.35cm, the ratio is calculated to be around 9.1. Therefore, the cell size is selected as 0.35cm and it falls within the recommended range of  $D^*/x$  values. In order to verify that the given mesh creates accurate results in FDS, a validation study is carried out with the same  $D^*/x$  ratio. The numerical grid distribution can be seen in Figure 4.3.

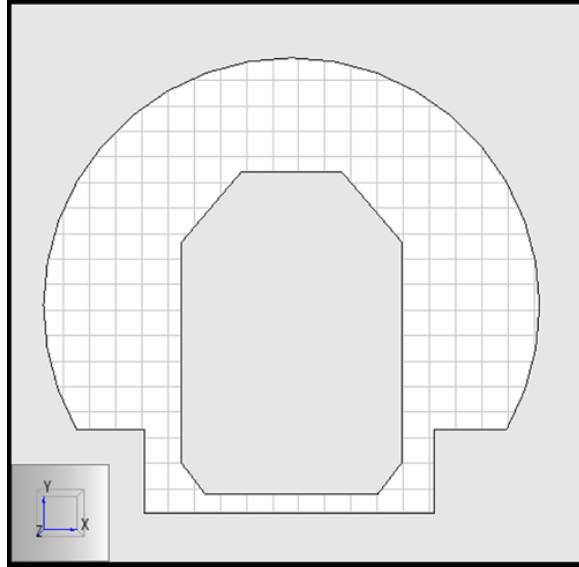


Figure 4.3: Cross-Sectional View of the Mesh

#### 4.1.2 Time Step

In order to solve partial differential equations described in Section 2.1.1, FDS uses finite volume method, and time, along with the volume has to be discretized. The time step is needed to be small enough to prevent numerical instabilities, but decreasing the time step increases the computation time drastically. Therefore, each time step has to be optimized for accuracy and computation time.

Time step in Fire Dynamics Simulator is calculated and updated automatically. The choice of time step depends strictly on the mesh size and in order to determine a suitable time step which guarantees stability, Courant–Friedrichs–Lewy (CFL) stability criterion is used. Time step is selected such that the CFL criterion is satisfied at every iteration. The CFL criterion is given by

$$\frac{u_x \Delta t}{\Delta x} + \frac{u_y \Delta t}{\Delta y} + \frac{u_z \Delta t}{\Delta z} < 1 \quad (4.2)$$

Table 4.1: Boundary Conditions

Description	Boundary Condition Type	Value
Tunnel Inlet	Velocity Inlet	3.80 m/s, 24.1°C
Cross Passage Inlet	Velocity Inlet	4.24 m/s, 24.1°C
Tunnel Walls	Stationary Wall	Adiabatic, No Slip
Train Walls	Stationary Wall	Adiabatic, No Slip
Tunnel Outlet	Pressure Outlet	0 Gage Pressure

where  $\Delta t$  denotes the time and  $u$ ,  $v$  and  $w$  represent the magnitude of velocity in  $x$ ,  $y$ , and  $z$  directions, respectively. Since every time step satisfies this condition, the solution of equations are never updated with a time step larger than that which would allow a fluid particle to travel more than a single mesh cell.

#### 4.1.3 Boundary Conditions

Appropriate boundary conditions are essential in obtaining meaningful numerical solutions. Tunnel inlet velocity is determined by on-site measurements, along with the inlet velocity at the cross passage entrance and these values are directly applied to the simulation. The fire is initiated at  $t = 0s$ , and for the first case, fans are operated at  $t = 120s$  since the activation of fire alarm and ventilation system requires some time whereas for the second case fans are not operated. Tunnel outlet is set to zero gage pressure. Tunnel and train walls are modeled with no slip boundary condition and they are assumed to be adiabatic. Other heat transfer options could be adopted for the tunnel walls but this is not a bad approximation since the tunnel linings are made of thick concrete material. Investigation of this assumption can be a subject of future research. This assumption also considers the worst case scenario since the heat transfer through the outer boundaries are neglected. Therefore, there will be no heat loss to the surroundings and all the thermal energy will be kept in the tunnel. The boundary conditions are summarized in Table 4.1.

The initial temperature inside the tunnel was set to 24.1°C in accordance with site measurements and the supply air temperature was also set to the same temperature.

During the second simulation, the same boundary conditions are used except the tunnel inlet and cross passage inlet velocities. For the case without fan activation, the

Table 4.2: Growth Factors Used In Previous Studies

Researcher	Fire Heat Release Rate	Alpha ( $W/s^2$ )	Year
Andrew Purchase et al.	5 MW	12	2017
Aram Amouzandeh et al.	25 MW	31	2014
Serkan Kayılı and Cahit Eralp	6 MW	47	2011
Francesco Colella	35 MW	245	2010
Shorab Jain	16 MW	300	2010
Jae Seong Roh	35 MW	385	1995

velocity inlets are defined as pressure outlets during the set up of the simulation.

## 4.2 Modeling of Fire

### 4.2.1 Fire Growth

The fire starts with the ignition and grows consuming the available fuel until it reaches the fully developed stage. Therefore, the growth of the fire from 0 to 20MW needs to be modeled in the simulation. A commonly used approximation is to use a t-squared method where the heat release rate is assumed to be growing proportionally with the square of time. This is one of the most valid approximations since the initial growth period is nearly always accelerating. The following equation defines the fire heat release rate of a growing fire as

$$\dot{Q} = \alpha \cdot t^2 \quad (4.3)$$

where  $\dot{Q}(kW)$  is the fire heat release rate,  $\alpha(kW/s^2)$  is the growth factor and  $t(s)$  is the time elapsed after the start of the fire, i.e. ignition.

The latest version of NFPA204 classifies fires according to their growth factors. A fire with growth factor of  $187 W/s^2$  is a very fast,  $46.9 W/s^2$  is a fast,  $11.7 W/s^2$  is a medium and  $2.9 W/s^2$  is a slowly growing fire. Figure 4.4 shows the growth rates for different fire growth factors. There is no specific growth rate given for the metro trains in the literature and it is expected to change based on the type of material used for the train. However previous researchers used different values of growth factor to carry out their simulations. Table 4.2 summarizes the growth factors previously used in metro train fire simulations. In early metro cars, the fire resistance of the material

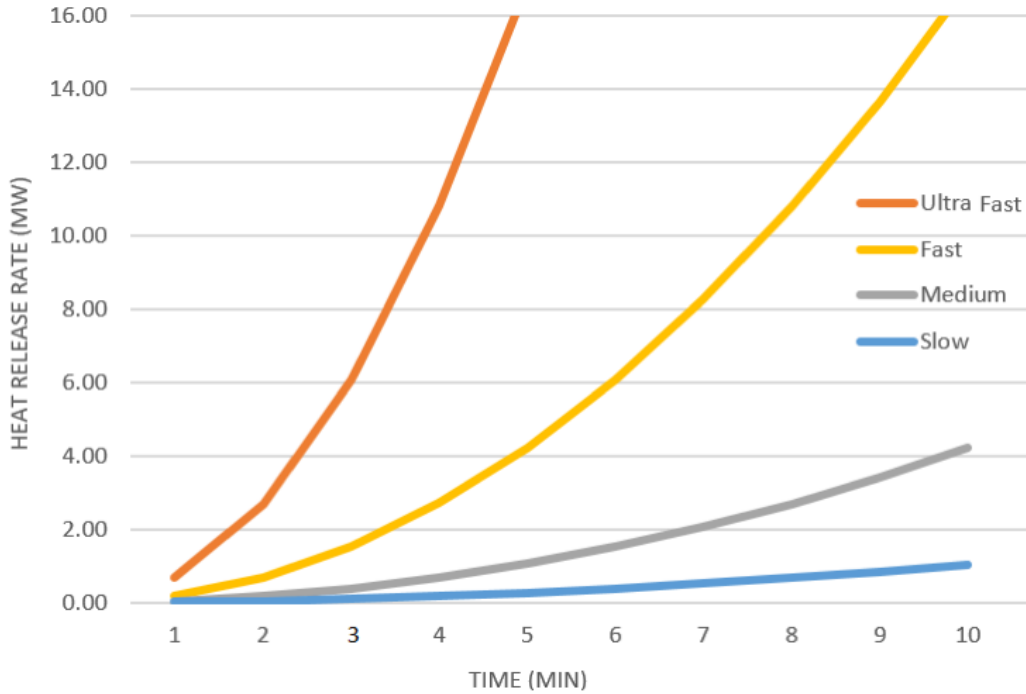


Figure 4.4: Heat Release Rate for Different Growth Factors

used was very low, moreover highly flammable materials were used for the seats, thermal insulation, etc. After the recent fire catastrophes in the metro tunnels, with the increased awareness of train fires, current trains cars are composed of higher fire rated materials, therefore alpha values used in modern simulations are considerably lower than the previous studies.

In this study, fire growth factor of  $46.9 W/s^2$  is used which corresponds to a fast fire growth rate. Therefore, it is assumed that the fire reaches its maximum rate of  $20MW$  in 654 seconds.

#### 4.2.2 Fire Characteristics

The fire is modeled at the bottom and two sides of the third train car at the mid-section. In previous fire cases which are explained in Section 1.2, it is seen that the flammable hydraulic fluid, or the wires located under the train might be the cause of the fire initiation. The fire can grow underneath the train since enough flammable materials are available. Therefore the burning area is modeled to be at the bottom part of and two sides of the middle car. The burning area can be seen in Figure 4.5. The

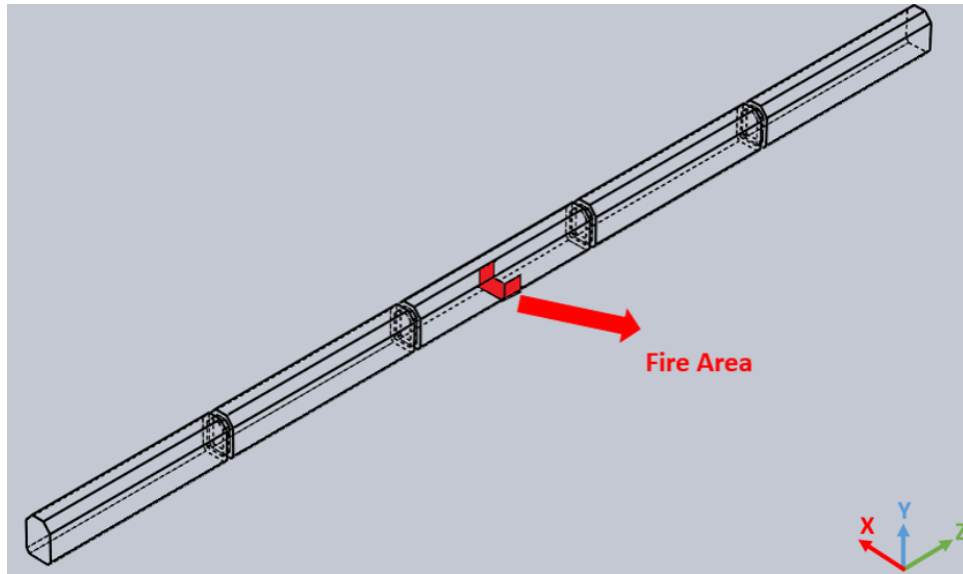


Figure 4.5: Fire Location on the Train

heat release rate of the fire follows the t-squared approximation and reaches a maximum value of  $20MW$ , and a fire area of  $12m^2$  is selected to represent the fire source distributed evenly on the bottom and sides of the train. Therefore, a maximum heat release rate of  $1666.7kW/m^2$  is defined for the burning surface area. The heat release rate starts from  $0kW/m^2$  at the start of the simulation and reaches its maximum value at  $t = 654$  seconds. Spread of fire is not modeled for simplicity and it is assumed that the fire location remains the same throughout the simulation.

Heptane is used as the source of fuel since it is a generic hydrocarbon fuel defined in Fire Dynamics Simulator. However the soot yield value is updated as  $0.117kg/kg$  to match the actual metro train conditions due to reasons explained in Section 2.1.3.



## CHAPTER 5

### SIMULATION RESULTS

The results are obtained for the given fire scenario as contour plots of temperature, visibility and velocity along the critical evacuation paths. Also the result of the validation study is explained in this chapter.

#### 5.1 Validation Results

Over the past decade, many validation studies have been carried out in order to determine the accuracy of Fire Dynamics Simulator and validation studies on full scale fire experiments showed that a  $D^*/\delta x$  ratio of 5 to 10 produces accurate results [22].

In order to validate the current study, experimental data obtained from scaled tunnel fire experiments by Serkan Kayılı [15] have been used. Serkan Kayılı carried out tests in 1/13 scale down model of bored tunnel in Istanbul Metro System at different ventilation velocities, blockage ratios and heat release rate. Test set-up is was built in the Mechanical Engineering Department of Middle East Technical University and it can be seen in Figure 5.1. Serkan Kayili measured the heat release by making use of oxygen consumption calorimetry and recorded his results throughout the simulation. The maximum heat release rate was measured to be 68kW. By making use of 27 different thermocouples located in different locations of the tunnel, he was able to compare the effects of heat release rate and air velocity on temperature distribution.

For validation purposes, the experimental set-up is modeled with the same dimensions and boundary conditions. The mesh is constructed of 12.100 elements so that the  $D^*/\delta x$  ratio is equal to the value in the full scale simulation carried out in this thesis



Figure 5.1: Experimental Setup of Scaled Tunnel

which is 9.1. The scaled model and thermocouple location can be seen in Figure 5.2. Inlet velocity boundary condition is applied at the inlet as  $1m/s$  in accordance with

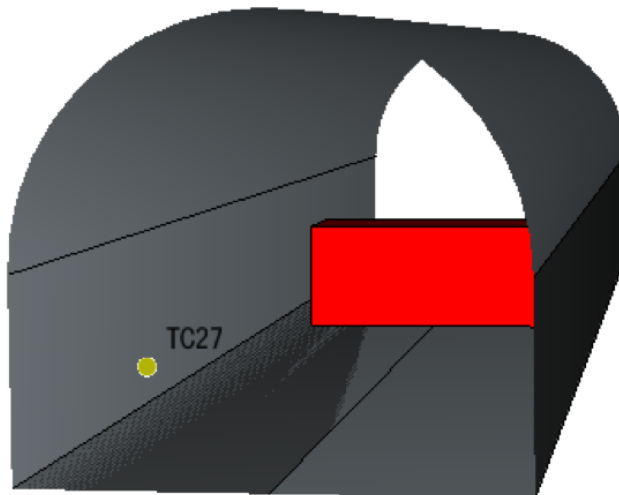


Figure 5.2: Section View of Scaled Tunnel Model

the experiment and the heat release rate from the fuel is set to the values measured by Serkan Kayili. Adiabatic wall boundary conditions were applied at the walls since the walls of the set-up is thermally insulated as well. The temperature values obtained by the simulation from “Thermocouple 27” were recorded and compared with the results from the experiments. Below graph (Figure 5.3) shows the simulation and

experimental results. Results show that even though the FDS simulations overshoot

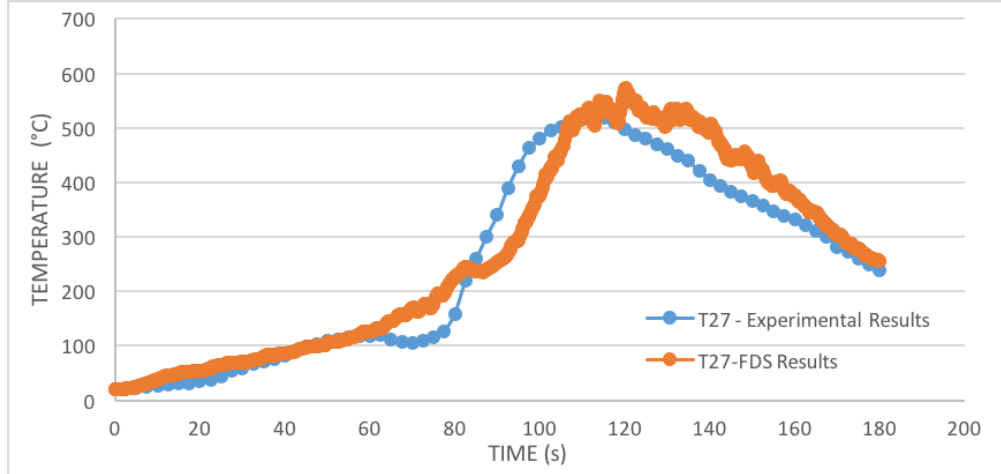


Figure 5.3: Comparison of FDS Results and Experimental Results

the temperature values by 15% at the peak temperatures, the overall trend is in line with the experimental results. Overestimation of the temperatures at high heat release rates can be caused by the adiabatic wall boundary conditions. Therefore for purposes of tenability assessment in the tunnel, FDS can be used with  $D^*/\delta x$  ratio of 9.1.

## 5.2 Temperature Contours

Contours of temperature are obtained at different times at a height of 1.80m from the walkway level ( $y = 3.7m$  plane). The plane from which the contours are obtained can be seen in Figure 5.4.

The passengers will be evacuating the fire zone through the walkways therefore the temperature above the walkways need to be evaluated carefully during the evacuation period. The temperature inside the tunnel increases with height due to the buoyancy effect of the hot air and soot, therefore in order to see the worst case scenario, the height of 1.80m is selected as the measurement plane height.

Results are given with 60 second intervals in order to clearly observe the temperature behavior inside the tunnel. Temperature scale of minimum temperature of 30°C to maximum temperature of 80°C is used for all plots for ease of comparison of temperatures at different times.

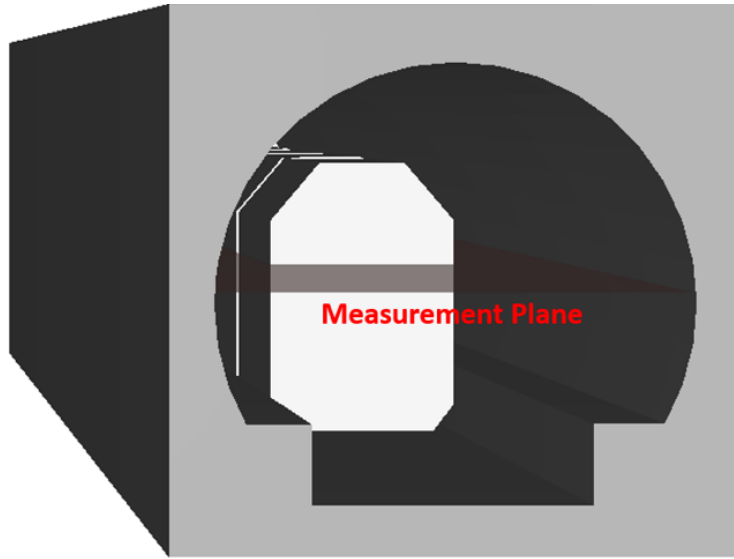


Figure 5.4: Measurement Plane at  $y = 3.7m$

Two different scenarios are plotted. In the following figures, Figure 5.5-5.9, the first contour is taken from the scenario with fan operation starting at  $t = 120s$  and the second contour is taken from the scenario with no fan operation. During the check for tenability criteria, it is important that the temperatures at the walkways and the cross-passage remain below  $60^{\circ}C$  throughout the evacuation time.

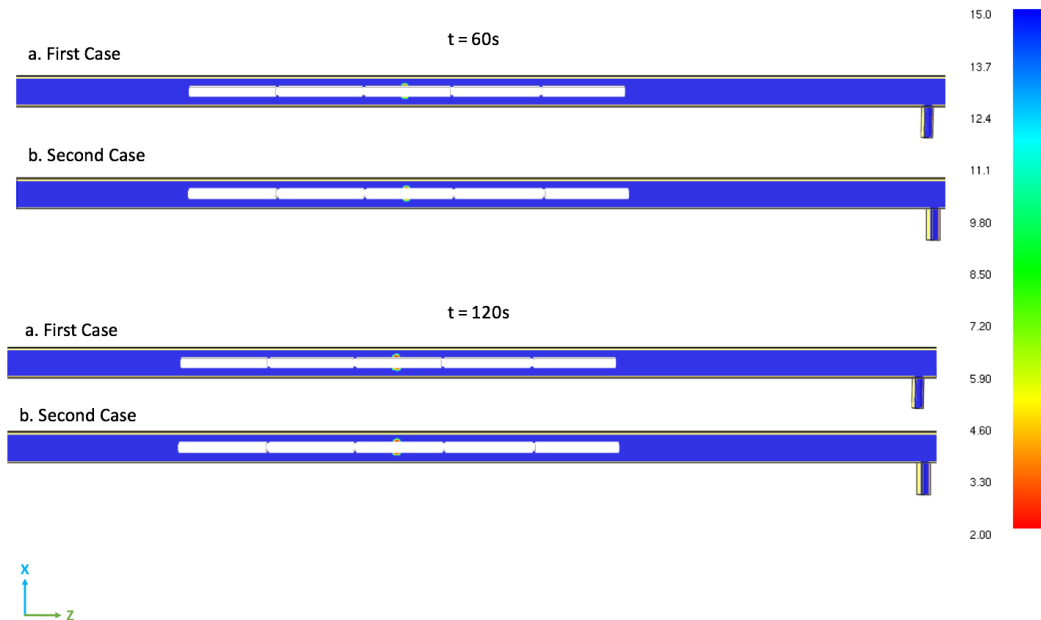


Figure 5.5: Temperature Distribution at  $y = 3.7m$  plane – a. with fan operation at  $t = 120$  seconds, b. with no fan operation

The simulation is carried for 600 seconds and the temperature plots are obtained as

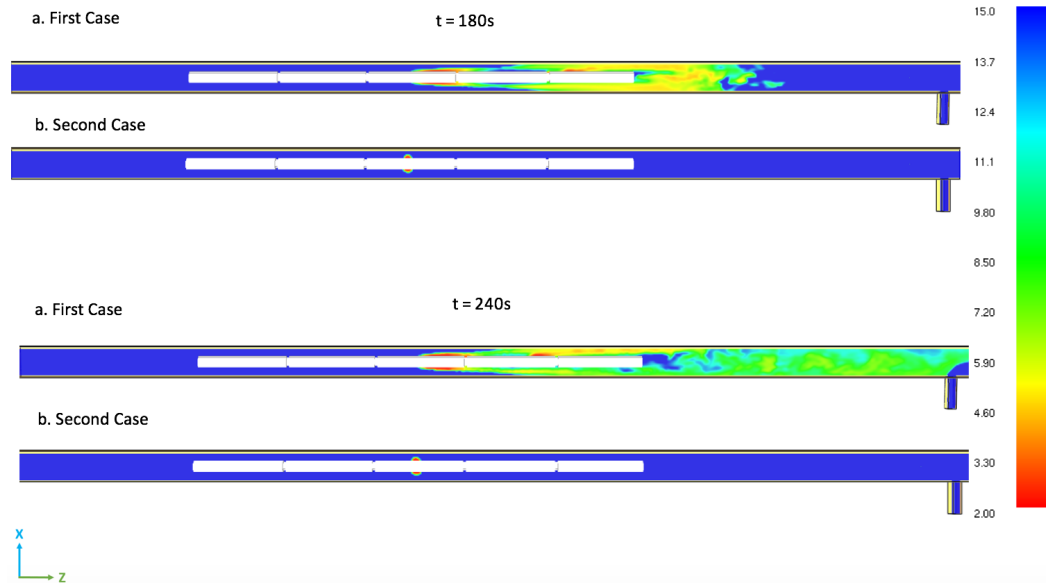


Figure 5.6: Temperature Distribution at  $y = 3.7m$  plane – a. with fan operation at  $t = 120$  seconds, b. with no fan operation

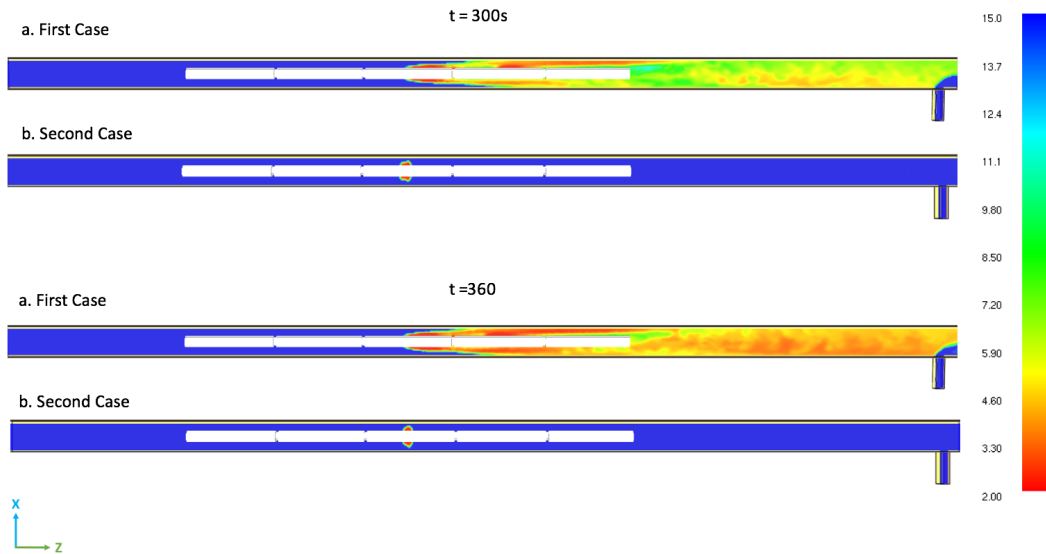


Figure 5.7: Temperature Distribution at  $y = 3.7m$  plane – a. with fan operation at  $t = 120$  seconds, b. with no fan operation

depicted in the above figures for both of the cases. It is obvious that during the first two minutes no significant temperature rise is observed since the heat release rate of the fire is very low. This is the reason why emergency alarm is delayed and fan operation starts 2 minutes into the simulation in the first case.

Fire heat release rate increase proportionally to the square of time, therefore the temperatures in the tunnel increase drastically as the simulation time increases for both

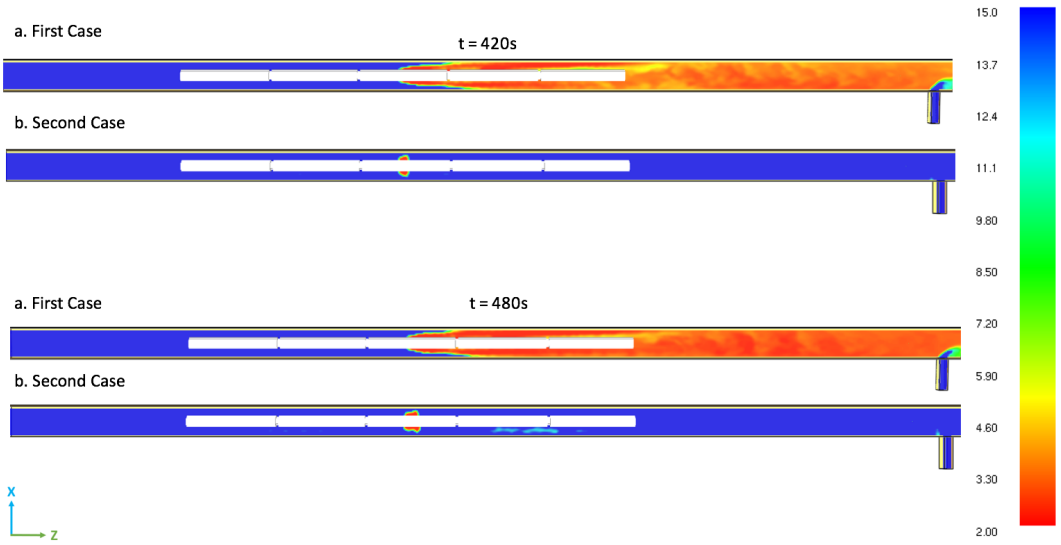


Figure 5.8: Temperature Distribution at  $y = 3.7m$  plane – a. with fan operation at  $t = 120$  seconds, b. with no fan operation

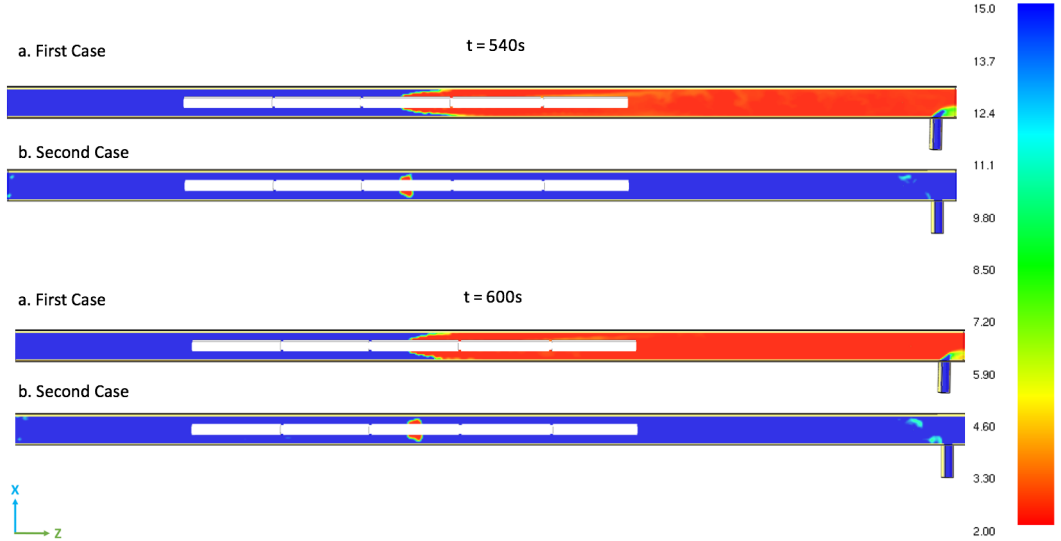


Figure 5.9: Temperature Distribution at  $y = 3.7m$  plane – a. with fan operation at  $t = 120$  seconds, b. with no fan operation

simulation results.

In the first case, with fan activation after the  $2^{nd}$  minute it is observed that backlay-  
 ering is prevented and the upstream side of the train is kept clear of smoke and hot  
 gasses throughout the entire simulation time. All the smoke is pushed to the down-  
 stream part of the train and as time passes, due to the increase in heat release rate,  
 downstream temperature starts to rise. Tunnel Ventilation System is capable of keep-

ing the temperature on both upstream and downstream side of the train below 50°C during the first four minutes of the simulation. By the end of fifth minute, heat release rate exceeds the value of 4MW and temperatures downstream of the fire at the walkways reach up to 60°C at a few locations and start risking the tenability in the tunnel. At 6th minute, these locations start growing and it is observed that walkway next to fourth car reaches to temperatures of 70°C whereas the last train car and rest of the escape routes remain at tenable temperatures. At the end of 7<sup>th</sup> minute, temperatures reach the value of 70-80°C at the escape routes downstream of the train. The temperature at the entire walkway is above 70°C and passengers who have not evacuated by the end of 7<sup>th</sup> minute are under great danger. It is important to note that throughout the simulation the upstream part of the tunnel is kept clear of smoke and passengers in the first three train cars can self-rescue without any threat of untenable environment.

On the other hand in the case without fan activation, it is seen that backlayering occurs and the hot gasses are distributed symmetrically towards the upstream and downstream directions. However, it is important to note that during the first six minutes due to the buoyancy effect, hot gasses stay at the ceiling reservoir of the tunnel and evacuation paths of the passengers are kept clear of hot gasses and temperatures never exceed 60°C below the height of 1.80m. By the end of the seventh minute, as the ceiling temperature increase, and the reservoir is filled up, temperature values at the walkway increase on both upstream and downstream sides of the tunnel symmetrically and exceeds the value of 60°C throughout the length of the train. Therefore, the area around all five cars are no longer tenable at the 7<sup>th</sup> minute. However, it is observed that upstream and downstream part of the train is still at low temperatures thus allows safe evacuation and the only untenable area is the train area which is 122m long.

Therefore, it is understood that both case 1 and case 2 have advantages over each other but the optimum ventilation mode needs to be decided in order to be applied in train fire scenarios.

In case one, passengers in the first three train cars can evacuate very easily without any threat however since the smoke is directed to the downstream, passengers at remain-

ing two train cars are subject to gasses with combustion products. The passengers at the last two cars need to either cross the fire zone to evacuate the tunnel through the upstream direction into the station, or they need to walk 80 meters downstream and evacuate through the cross passage within the first 6 minutes.

Whereas in the second case passengers have two extra minutes to evacuate the tunnel but since backlayering is not prevented, high temperatures are seen both at the upstream and downstream of the fire zone thus possibly creating minor injuries, or threatening the lives of the last evacuees.

Therefore, in case of a mid-tunnel ventilation, all the passengers should be directed to the upstream side for safe evacuation and the fan operation should be delayed until all passengers are upstream side of the fire. Once all the passengers are safely on the upstream side, only then the fans should be started to prevent backlayering and assists evacuation.

### **5.3 Contours of Visibility**

As the fire size increases, more fuel is turned into soot which fills up the tunnel and adversely effects visibility. In order to assess the minimum 5m visibility criteria, contours of visibility were plotted on a plane which is 1.8m above the walkway level ( $y = 3.7m$  plane). The height is selected above the average human height in order to account for worst case conditions. In the shown snapshots, Case 1 corresponds to the scenario with fan operations starting at  $t = 120$  seconds whereas Case 2 represents the scenario with no fan activation throughout the entire scenario. The simulation was carried out for 600 seconds and plots were obtained at every 60 seconds as shown below:

The simulation is carried out for 600 seconds and the visibility plots are obtained as depicted in the above images for both the cases with ventilation system operating and not operating.

For the first case it is seen that the smoke layer is undisturbed until the end of 2<sup>nd</sup> minute on which the fans are operated. After the fan operation, since backlayering

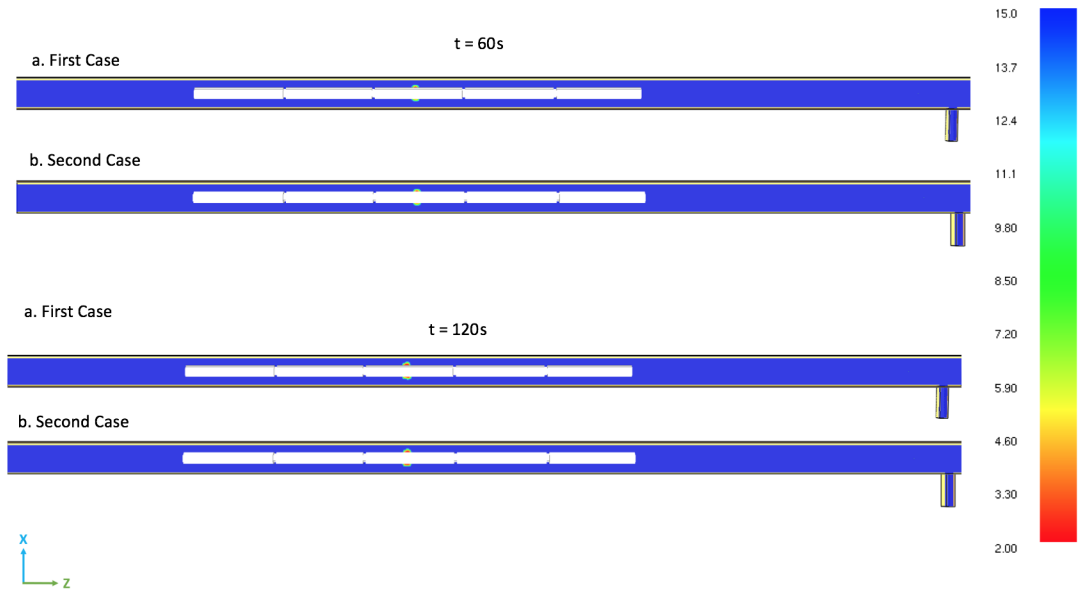


Figure 5.10: Visibility Plot at  $y = 3.7m$  plane – a. with fan operation at  $t = 120$  seconds, b. with no fan operation

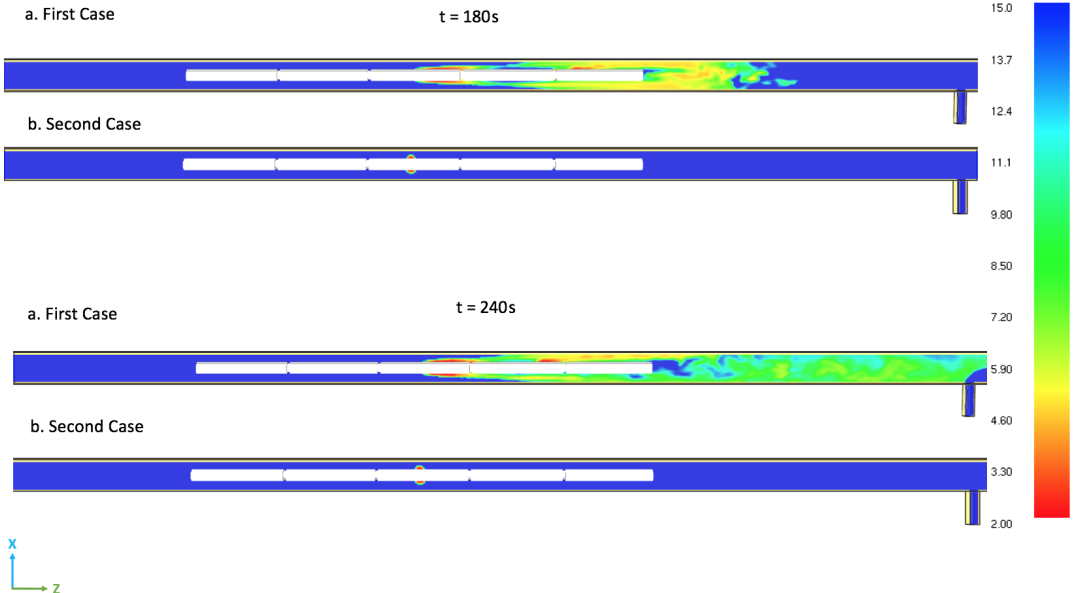


Figure 5.11: Visibility Plot at  $y = 3.7m$  plane – a. with fan operation at  $t = 120$  seconds, b. with no fan operation

is prevented, upstream of the fire is kept clear throughout the remainder of the simulation. However, all the soot particles are directed towards the downstream side of the fire and the smoke stratification at the ceiling is disturbed with the fresh incoming air. Fresh air and smoke particles mix and the temperature difference between the

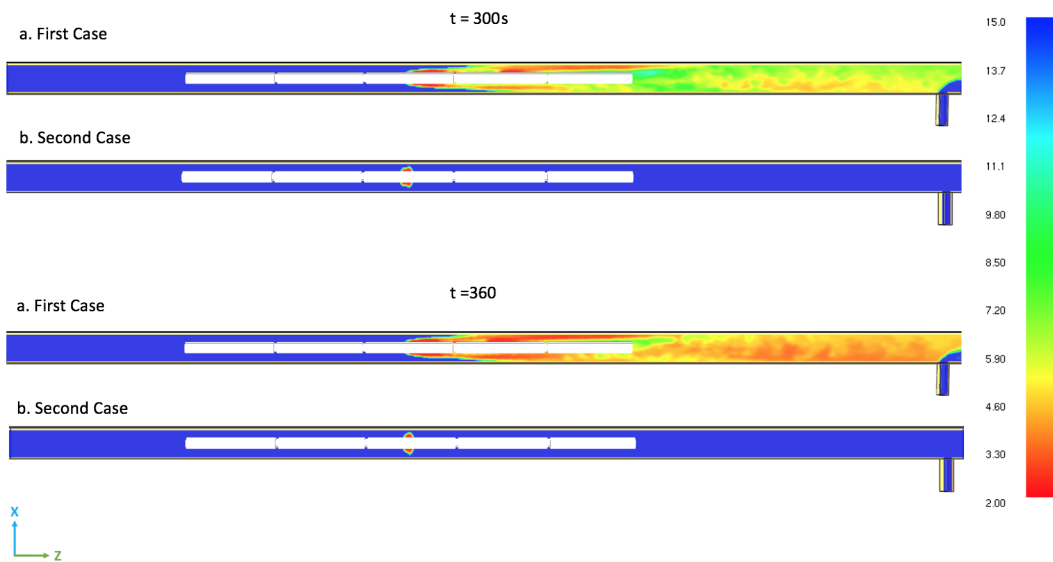


Figure 5.12: Visibility Plot at  $y = 3.7m$  plane – a. with fan operation at  $t = 120$  seconds, b. with no fan operation

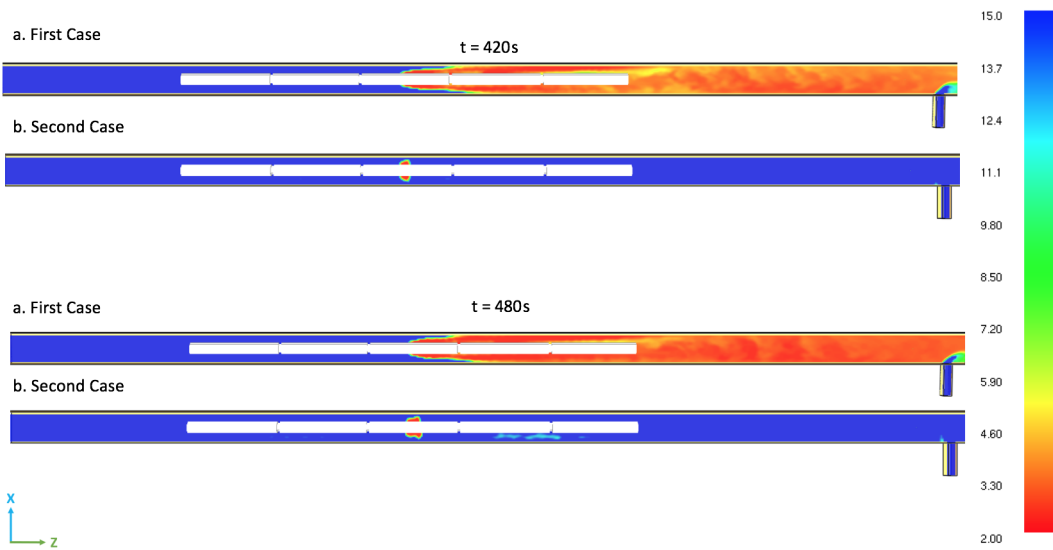


Figure 5.13: Visibility Plot at  $y = 3.7m$  plane – a. with fan operation at  $t = 120$  seconds, b. with no fan operation

air and smoke diminishes causing the smoke to descend and cover the entire tunnel area. Visibility is greater than  $5m$  during the first 5 minutes but during the  $6^{th}$  minute visibility values at the walkways decrease to values below  $5m$  and the evacuation is endangered. It is also observed that the fresh air coming from the cross-passage keeps the walkway area clean of smoke at the location where two streams interface.

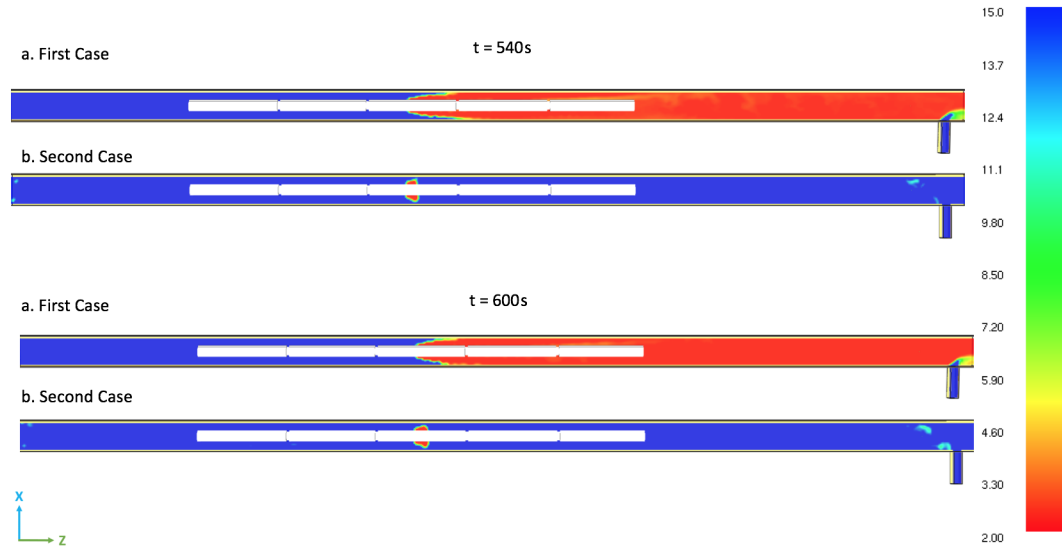


Figure 5.14: Visibility Plot at  $y = 3.7m$  plane – a. with fan operation at  $t = 120$  seconds, b. with no fan operation

On the second case, without the fan activation it is observed that the smoke particles stay close to the ceiling and does not descend below the height of  $1.80m$ . This is mainly due to the temperature difference between the hot soot particles and the air present in the tunnel. Since the tunnel has a large reservoir above the plane height, the soot particles take long time to fill up the upper layers and they move evenly along both directions in the tunnel. It is seen that even at the maximum heat release rate of the fire at the  $10^{th}$  minute, visibility stays above  $5m$  and safe evacuation is not endangered.

#### 5.4 Temperature Graphs

To be able to clearly compare the tenability of two cases, in the FDS Simulation, thermocouples are located over the center of the walkway at a height of  $1.80m$  ( $y = 3.7m$  plane) with  $5m$  spacing in between. The temperatures are measured every second and the data was recorded. Temperature values were averaged over 10 seconds in order to avoid rapid fluctuations and the results for  $6^{th}$  and  $7^{th}$  minute were plotted in the below figures (Figure 5.15-5.16). The red line shows the limit of  $T = 60^{\circ}C$  and it is assumed that tenable conditions no longer exists above this value. In the below figures (Figure 5.15-5.16) Case 1 represents the case with Tunnel Ventilation System oper-

ation whereas Case 2 represents the scenario without the fan activation. The fire is located at the 105<sup>th</sup> meter inside the tunnel and cross-passage is located at the 235<sup>th</sup> meter.

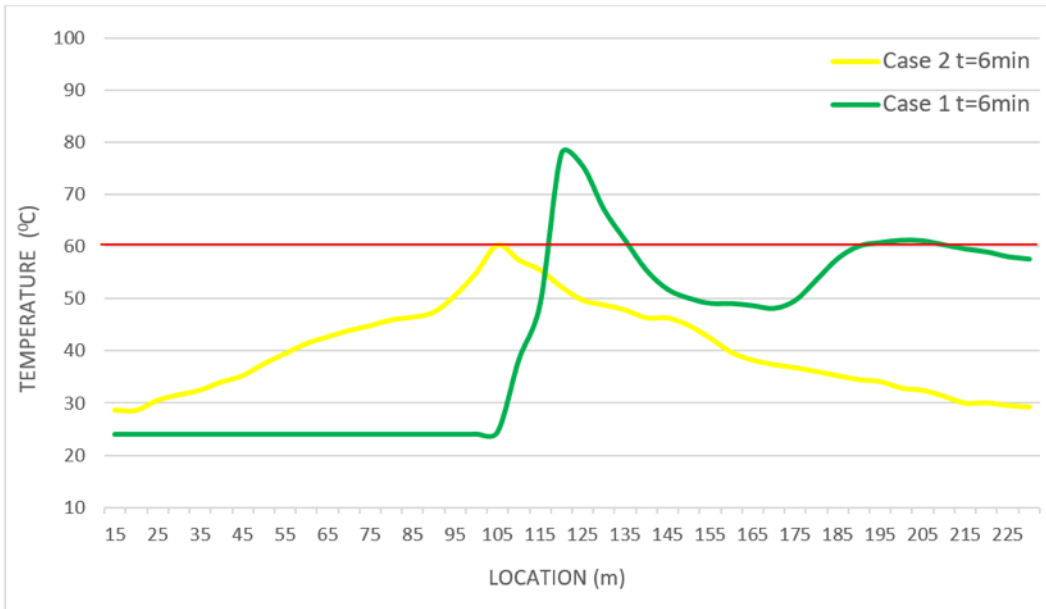


Figure 5.15: Comparison of Walkway Temperature Distribution With and Without Fan Operation at 6<sup>th</sup> Minute

The graph (Figure 5.15) clearly shows that during the 6<sup>th</sup> minute, ventilation inside the tunnel prevents backlayering and keeps the upstream direction at low temperatures, however the temperatures at the downstream side reach to high values since the entrained fresh air disturbs the stratified smoke later and causes it to descend below the height of 1.80m. On the other hand, without the fan activation it is observed that the hot gasses stick to the ceiling and no temperature hazard is present at human height. Hot gasses move symmetrically to the upstream and downstream sides. Figure 5.16 shows the situation at the 7<sup>th</sup> minute:

For Case 1, it is observed that the tenability limit is not satisfied anywhere at the downstream of the fire and the lives of the passengers still remaining at the downstream part of the train or walkways at the 7<sup>th</sup> minute is under great risk. On the contrary for Case 2 it is seen that tenability limits are exceeded at only a limited area around the fire. This untenable area occurs between 80<sup>th</sup> to 140<sup>th</sup> meters and this is acceptable by international standards [3], since it is impractical to apply tenability

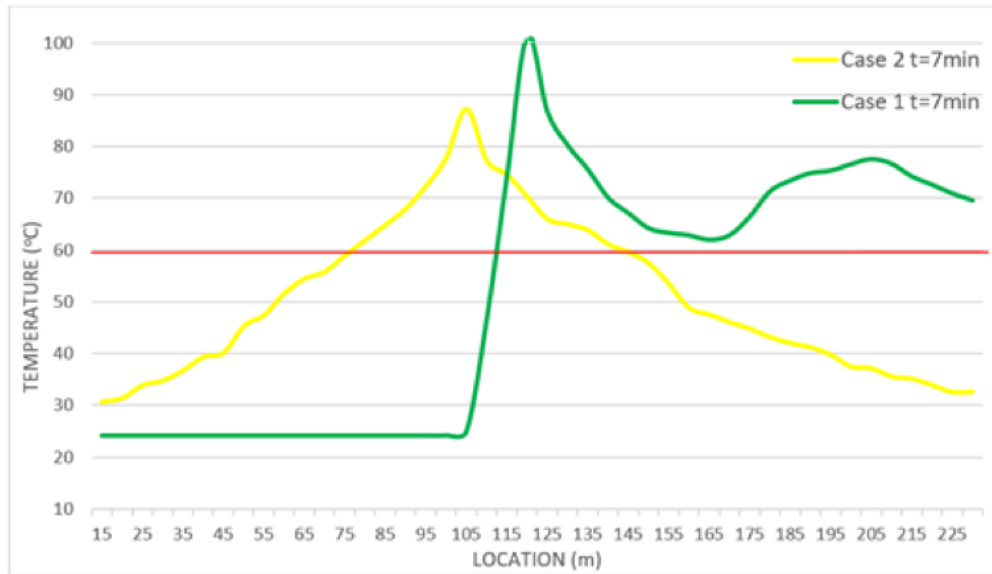


Figure 5.16: Comparison of Walkway Temperature Distribution With and Without Fan Operation at 7<sup>th</sup> Minute

criteria at the perimeter of fire and the zone of tenability should be applied roughly 30m away from the fire location.

As time passes, due to the increase of heat release rate higher temperatures are observed in the tunnel and the temperatures for Case 2 exceed the tenability limit after the 8<sup>th</sup> minute.



## CHAPTER 6

### DISCUSSION AND CONCLUSION

#### 6.1 Discussion About the Results

The most critical case in tunnel fires is the fire in the middle of the train and this situation was investigated for the Ayrılıkçeşmesi Station of the Istanbul Metro Line. Two cases were investigated, in the first case, the Tunnel Ventilation System was operated during the detection of fire ( $t = 120s$ ) as planned in the SES Fire Scenario whereas in the second case, ventilation systems were not activated throughout the simulation.

The ventilation direction is determined in SES simulations carried out by Tunnel Ventilation System Designers, as directed from the Ayrılıkçeşmesi Station towards the tunnel and the velocity is above the critical velocity. Therefore, with the activation of the Tunnel Ventilation System, the front three train cars are cleared from smoke and hot gasses but the ventilation pushes the combustion products to the downstream side of the train and remaining three train cars and the walkways are subject to untenable environments. After the fan operation, it is observed that no backlayering occurs, i.e, the passengers at the upstream side of the fire can self-evacuate easily through the walkway and into the Ayrılıkçeşmesi Station. It is seen that after the sixth minute of fire ignition, both temperature and visibility criteria are failed, therefore the lives of passengers remaining at the downstream side of the fire are threatened after the sixth minute.

On the other hand if the fans are not operated, the hot gasses tend to stack at the upper layers and do not threaten the evacuation during the first seven minutes. Therefore,

compared to the first case, passengers have an extra 80-90 seconds before the temperature limits are exceeded in the case where fans are not operated. It is also important to note that visibility limit is never exceeded for this case since the hot gasses remain at the upper parts of the tunnel and cannot fill the reservoir throughout the simulation.

The adiabatic heat transfer assumption on the tunnel walls has also an effect on the temperature plots and it can be said that the temperature values would be lower in a real fire case due to the heat transfer through the tunnel walls thus tenability time would increase slightly.

Tunnel Ventilation Systems are very efficient during end train and front train fires, and they provide tenable environment for all passengers if they are operated in the right manner. On the other hand, during the mid-tunnel fire cases it is observed that ventilation activation has an adverse effect for the passengers on the downstream side of the fire therefore fans should not be operated until evacuation at downstream side is completed. After evacuation, the fans shall be operated to create safe and smoke free access for the firefighters.

Previous accidents show that improvements are required to prevent loss of lives in Metro Train Fires. Following improvements can be made in order to further increase the safety degree in case of Tunnel Fires in Underground Metro Systems:

- Informing passengers about evacuation scenarios by signs or TV screens in the train cars.
- Carrying out frequent fire drills to train the personnel
- Installation of Safe Rooms on the walkways between cross-passages
- Applying transverse ventilation instead of longitudinal ventilation throughout the tunnel network.

## **6.2 Recommendations for Future Work**

Underground Metro Systems are rapidly expanding throughout the entire world and tunnel fires will be one of the important topics of the next decades. This study aimed to create a full scale simulation of a mid-tunnel train fire by making use of the bound-

ary conditions obtained in on-site measurements. Further improvements can be made by the future researchers:

- The adiabatic tunnel wall assumption can be investigated by expanding the mesh and modeling the concrete walls of the tunnel.
- The evacuation time can be calculated by making use of a software such as Evac and a detailed tenability analysis can be carried out.
- Sprinkler Systems are used in some countries to fight the tunnel fires. The effects of sprinkler systems on train fires and the cost impact can be investigated.
- Instead of widely used Longitudinal Ventilation, a Transverse Ventilation System can be modeled and the results can be analyzed.



## REFERENCES

- [1] F. ASHRAE. Fundamentals handbook. *IP Edition*, 2013.
- [2] H. A. S. H. ASHRAE. Hvac applications handbook. *IP Edition*, 2011.
- [3] N. F. P. Association et al. *NFPA 130: Standard for Fixed Guideway Transit and Passenger Rail Systems*. NFPA, 2003.
- [4] A. Beard, R. Carvel, et al. *The handbook of tunnel fire safety*. Thomas Telford London, 2005.
- [5] B. Benkoussas, A. Bouhdjar, and O. Vauquelin. Numerical security assessment in case of fire in underground transport spaces. *Nature & Technology*, (12):45, 2015.
- [6] W. Binbin. Comparative research on fluent and fds's numerical simulation of smoke spread in subway platform fire. *Procedia Engineering*, 26:1065–1075, 2011.
- [7] R. O. Carvel. Fire size in tunnels. 2004.
- [8] F. Chen, S.-C. Guo, H.-Y. Chuay, and S.-W. Chien. Smoke control of fires in subway stations. *Theoretical and computational fluid dynamics*, 16(5):349–368, 2003.
- [9] B. H. Chiam. Numerical simulation of a metro train fire. 2005.
- [10] S. Cochard. Validation of the freeware 'fire dynamics simulator version 2.0' for simulating tunnel fires. *Tunnel Management International Journal*, 6(4):32–37, 2003.
- [11] S. Gaillot, A. Revell, D. Blay, J.-P. Vantelon, and P. Deberteix. Contribution to the control of fire-induced smoke flow in longitudinally ventilated tunnels. *Fire Safety Science*, 8:1449–1460, 2005.
- [12] H. Ingason, Y. Z. Li, and A. Lönnemark. *Tunnel fire dynamics*. Springer, 2014.
- [13] T. Jin. Studies on human behavior and tenability in fire smoke. *Fire Safety Science*, 5:3–21, 1997.
- [14] S. Kayili. *CFD simulation of fire and ventilation in the stations of underground transportation systems*. PhD thesis, Middle East Technical University, 2005.
- [15] S. Kayili. *Effect of vehicles' blockage on heat release rate in case of tunnel fire*. PhD thesis, PhD. Thesis, Department of Mechanical Engineering, Middle East Technical University, Ankara, Turkey, 2009.
- [16] S. Kayılı and O. Eralp. Yeraltı taşıma sistemleri istasyonlarında hesaplamalı akışkanlar dinamiği yöntemiyle yangın ve havalandırma simülasyonu. 8. *Ulusal Tesisat Mühendisliği Kongresi*, pages 25–28.

- [17] S. K. Li and W. D. Kennedy. A cfd analysis of station fire conditions in the buenos aires subway system. *Transactions-American Society of Heating Refrigerating and Air Conditioning Engineers*, 105:410–413, 1999.
- [18] I. Y. Maeviski. *Design fires in road tunnels*, volume 415. Transportation Research Board, 2011.
- [19] K. McGrattan and A. Hamins. Numerical simulation of the howard street tunnel fire. *Fire Technology*, 42(4):273–281, 2006.
- [20] K. McGrattan, S. Hostikka, R. McDermott, J. Floyd, C. Weinschenk, and K. Overholt. Fire dynamics simulator technical reference guide volume 1: mathematical model. *NIST special publication*, 1018(1):175, 2013.
- [21] E. Musluoğlu. *A theoretical analysis of fire development and flame spread in underground trains*. PhD thesis, Ph. D. Dissertations, Middle East Technical University Mechanical Engineering Department, 2009.
- [22] U. NRC. Verification and validation of selected fire models for nuclear power plant applications. *Nuclear Regulatory Commission, NUREG-1824*, 2007.
- [23] A. Purchase, K. Fridolf, and D. Rosberg. A comparative study of fire safety provisions effecting evacuation safety in a metro tunnel. 2016.
- [24] J. S. Roh, H. S. Ryou, W. H. Park, and Y. J. Jang. Cfd simulation and assessment of life safety in a subway train fire. *Tunnelling and Underground Space Technology*, 24(4):447–453, 2009.
- [25] R. Seigel and J. R. Howell. Thermal radiation heat transfer. *McGraw-Hill Book Co*, page 836, 1981.
- [26] M. Seike, N. Kawabata, and M. Hasegawa. Experiments of evacuation speed in smoke-filled tunnel. *Tunnelling and Underground Space Technology*, 53:61–67, 2016.
- [27] P. Thomas. The movement of buoyant fluid against a stream and the venting of underground fires. *Fire Safety Science*, 351:1–1, 1958.
- [28] P. H. Thomas. The movement of smoke in horizontal passages against an air flow. *Fire Safety Science*, 723:1–1, 1968.
- [29] M. Tsukahara, Y. Koshihara, and H. Ohtani. Effectiveness of downward evacuation in a large-scale subway fire using fire dynamics simulator. *Tunnelling and Underground Space Technology*, 26(4):573–581, 2011.
- [30] Y. F. Wang, T. Qin, X. F. Sun, S. Liu, and J. C. Jiang. Full-scale fire experiments and simulation of tunnel with vertical shafts. *Applied Thermal Engineering*, 105:243–255, 2016.
- [31] T. U. Yanali. *An Experimental Study on the Pool Fire Burning Characteristics of N-Heptane and Ethanol in the Tunnels*. PhD thesis.
- [32] A. Çelik. *Experimental and numerical studies on fire in tunnels*. PhD thesis, Middle East Technical University, 2011.

## APPENDIX A

### TEST REPORTS

Scenario Check List			
MECON	CHECKLIST (page 1)		
Site. <i>Ayvalıkçeşme</i>	Functional Description. <i>Tunnel Fire Scenario</i>		
Project. <i>Marmaray</i>	Location Drg. No.		
	Schematic Drg. No.		
Project No. <i>MAR-01</i>	Plant No. <i>T7-4 Track 1</i>		
Item Ref No. <i>MAR-01-T7-4</i>	System No. <i>T7-4</i>		
			<b>IQ</b>
	Yes	No	Date
<b>Fire Scenario T7-4</b>			
YVP is on shutdown. -TVF01, TVF02, TVF03 and TVF04 are off. -FID01, FID02, FID03 and FID04 are closed. -DRD01 is open. -SID01 and SID02 are open. -TID01 and TID02 are open.	✓		<i>24.07.14</i>
YNW is on shutdown. -TVF01, TVF02, TVF03 and TVF04 are off. -FID01, FID02, FID03 and FID04 are closed. -DRD01 is open. -TID01, TID02 and TID03 are open.	✓		
Yenikapı OTE's are off.	✓		
Yenikapı Metro Connections are open.	✓		
YTE is on shutdown. -TVF01, TVF02, TVF03 and TVF04 are off. -FID01, FID02, FID03 and FID04 are closed. -DRD01 is open. -TID01 and TID02 are open.	✓		
X14 is on shutdown. -JF01 and JF02 are off.	✓		
SKW is on shutdown.	✓		
Sirkeci OTE's are off.	✓		
Sirkeci South Fire Door and North Fire Doors are open.	✓		

Figure A.1: Scenario Checklist 1

MECON		CHECKLIST (page 2)		
Site. <i>Ayriboğesme</i>	Functional Description. <i>Tunnel Fire Scenario</i>			
Project. <i>Marmaray</i>	Location Drg. No.			
	Schematic Drg. No.			
Project No. <i>MAR-01</i>	Plant No. <i>T7-4 Track 1</i>			
Item Ref No. <i>MAR-01-T7-4</i>	System No. <i>T7-4</i>			
				<b>IQ</b>
	Yes	No	Date	
SKE is on shutdown.	✓			
UKW Works in position 61 means exhaust from T2. -TVF01, TVF02, TVF03 and TVF04 operate in exhaust mode. -FID01, FID02, FID03 and FID04 are open. -DRD01 is closed. -TID01 is closed and TID02 is open.	✓			
Üsküdar OTE's are off.	✓			
Üsküdar Fresh Air Openings are open.	✓			
UKE works in position 61 means exhaust from T2 -TVF05, TVF06, TVF07 and TVF08 operate in exhaust mode. -FID05, FID06, FID07 and FID08 are open. -DRD02 is closed. -TID03 is closed, TID04 is open.	✓			
X15 is on shutdown. -JF01, JF02, JF03, JF04, JF05, JF06 and JF07 are off.	✓			
AVP works in position 55 means supply to T1W & T2W Saccardo. -TVF01, TVF02, TVF03 and TVF04 operate in supply mode. -FID01, FID02, FID03 and FID04 are open. -DRD01 is closed. -SID01 and SID02 are open. -TID01 and TID02 are closed.	✓			
Comments	Signature			
	<i>M. Alper Üstüner</i>			<i>Y. Şanlı</i>
DECLARATION:	Date:	Signature:		

Figure A.2: Scenario Checklist 2

<b>MECON</b>	<b>TUNNEL VELOCITY (Scenario T7-4)</b>																		
Site. <i>Ayrılıkçayırme</i>	Functional Description: <i>Tunnel Fire Scenario</i>																		
Project. <i>Marmaray</i>	Location Drg. No.																		
Project No. <i>MAR-01</i>	Schematic Drg. No.																		
Item Ref No. <i>MAR-01-T7-4</i>	Plant No. <i>T7-4 Track 1</i>																		
	System No. <i>T7-4</i>																		
<b>TUNNEL VELOCITY</b>																			
<b>PQ</b>																			
Pressure Difference (Pa)	Velocity(m/s)																		
$\Delta P_1 = 104.1$ Pa	$v_1 = 4.14$ m/s																		
$\Delta P_2 = 104.55$ Pa	$v_2 = 4.23$ m/s																		
$\Delta P_3 = 44.3$ Pa	$v_3 = 2.65$ m/s																		
$\Delta P_4 = 61.43$ Pa	$v_4 = 3.30$ m/s																		
$\Delta P_5 = 104.85$ Pa	$v_5 = 4.29$ m/s																		
$\Delta P_6 = 104.36$ Pa	$v_6 = 4.19$ m/s																		
	$v_{average} = 3.8$ m/s																		
$v = \sqrt{\frac{2 \cdot \Delta P}{\rho}}$																			
DB = <i>26.1</i> °C																			
Rel Hum = <i>80</i> %																			
$\rho = 1.18$ kg/m <sup>3</sup> ( from psychrometric chart)																			
	<table border="1"> <thead> <tr> <th></th> <th>Design</th> <th>Actual</th> </tr> </thead> <tbody> <tr> <td>Tunnel Area (m<sup>2</sup>)</td> <td>33.26</td> <td><i>33.26</i></td> </tr> <tr> <td>Full Velocity (m/s)</td> <td>3.38</td> <td><i>3.8</i></td> </tr> <tr> <td>Volume flow rate (m<sup>3</sup>/s)</td> <td>112.42</td> <td><i>126.39</i></td> </tr> <tr> <td>Annular Area (m<sup>2</sup>)</td> <td>21.27</td> <td><i>21.27</i></td> </tr> <tr> <td>Calculated Annular velocity (m/s)</td> <td>5.28</td> <td><i>5.94</i></td> </tr> </tbody> </table>		Design	Actual	Tunnel Area (m <sup>2</sup> )	33.26	<i>33.26</i>	Full Velocity (m/s)	3.38	<i>3.8</i>	Volume flow rate (m <sup>3</sup> /s)	112.42	<i>126.39</i>	Annular Area (m <sup>2</sup> )	21.27	<i>21.27</i>	Calculated Annular velocity (m/s)	5.28	<i>5.94</i>
	Design	Actual																	
Tunnel Area (m <sup>2</sup> )	33.26	<i>33.26</i>																	
Full Velocity (m/s)	3.38	<i>3.8</i>																	
Volume flow rate (m <sup>3</sup> /s)	112.42	<i>126.39</i>																	
Annular Area (m <sup>2</sup> )	21.27	<i>21.27</i>																	
Calculated Annular velocity (m/s)	5.28	<i>5.94</i>																	
Test Instrument <i>Rig</i>	Serial No _____																		
Test carried out by: <i>M. Alper USTONER</i>	Sign: <i>[Signature]</i> Date: <i>24.07.14</i>																		
Test witnessed and results accepted by:	Sign: _____ Date: _____																		
Comments: Velocity in the middle of the ring is <i>4.5</i> m/s measured by TESTO 435-4 with the serial number <i>02617262</i> ...																			
<b>DECLARATION:</b> Data recorded above has been reviewed and found to be satisfactory	Sign: _____ Date: _____																		

Figure A.3: Tunnel Velocity

<b>MECON</b>		<b>WALKWAY VELOCITY</b>	
Site: <i>Ay. İhtiyaçları</i>		Functional Description: <i>Tunnel Fire Scenario</i>	
Project: <i>Marmaroy</i>		Location Drg. No.	
Project No. <i>MAR-01</i>		Schematic Drg. No.	
Item Ref No. <i>MAR-01-T7-4</i>		Plant No. <i>T7-4 Track 2</i>	
		System No. <i>T7-4</i>	
<b>DYNAMIC PRESSURE (Pa)</b>			<b>PQ</b>
Location Code:	DB= <i>24.6</i>	+ = Required measuring position	
	Rel Hum= <i>80</i> %	All measurements to be noted at	
	$\rho$ = <i>1.18</i> kg/m <sup>3</sup> ( at psycometric cart)	positions.	
Test Scenario:			
Average velocity m/s		Design	Actual
		<i>11</i>	<i>7.3</i>
While the measurement is being recorded, the opening must not be obstructed			
NOTE: Velocity to be measured using an electronic anemometer			
Test Instrument	<i>Testa 435-4</i>	Serial No	<i>02617268</i>
Test carried out by: <i>M. Alper ÜSTÜNER</i>		Sign: <i>[Signature]</i>	Date: <i>24.07.16</i>
Test witnessed and results accepted by:		Sign:	Date:
Comments:			
<b>DECLARATION:</b>		Sign:	Date:
Data recorded above has been reviewed and found to be satisfactory			

Figure A.4: Walkway Velocity

Page:

MECON		CROSS PASSAGE VELOCITY	
Site. <i>Ayrılıkcesme</i>	Functional Description: <i>Tunnel Fire Scenario</i>		
Project. <i>Marmaray</i>	Location Drg. No.		
	Schematic Drg. No.		
Project No. <i>MAR-01</i>	Plant No. <i>T7-4 Track 2</i>		
Item Ref No. <i>MAR-01-T7-4</i>	System No. <i>T7-4</i>		
<b>PQ</b>			
Location Code:	DB= <i>241C</i>	+ = Required measuring position	
	Rel Hum= <i>80%</i>	All measurements to be noted at	
	$\rho = 1.18 \text{ kg/m}^3$ ( at psychometric cart)	positions.	
Test Scenario:			
	Opening size	m <sup>2</sup> <i>31.53</i>	Actual <i>61.04</i>
	Average velocity	m/s <i>4.13</i>	<i>4.24</i>
	Volume flow rate	m <sup>3</sup> /s <i>141.6</i>	<i>171.2</i>
	While the measurement is being recorded, the opening <u>must not be</u> obstructed		
	NOTE: Velocity to be measured using an electronic anemometer		
Test Instrument	<i>Testo 435-4</i>	Serial No	<i>02617268</i>
Test carried out by:	<i>M. Aker ÖSTÖNER</i>	Sign:	<i>[Signature]</i> Date: <i>24.07.14</i>
Test witnessed and results accepted by:		Sign:	Date:
Comments:			
<b>DECLARATION:</b>		Sign:	Date:
Data recorded above has been reviewed and found to be satisfactory			

Figure A.5: Cross Passage Velocity

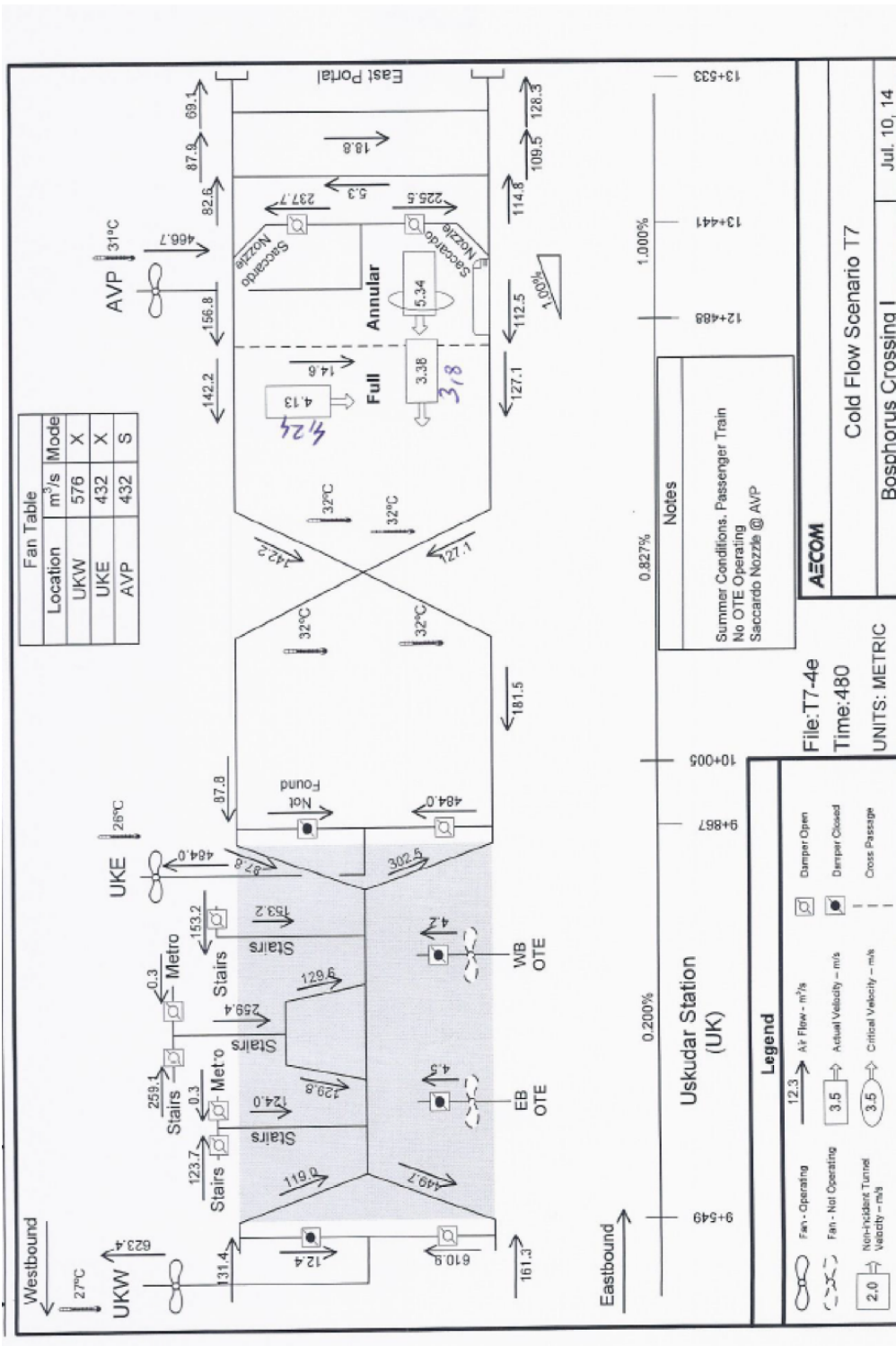


Figure A.6: Cold Flow Scenario